(2)

NAVAL POSTGRADUATE SCHOOL
Monterey, California

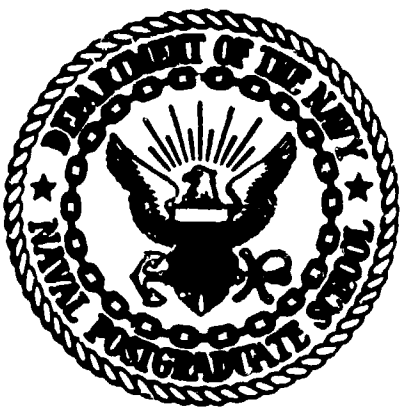

THESIS

STUDY OF ELECTROSTATIC MODULATION OF FUEL SPRAYS TO ENHANCE COMBUSTION PERFORMANCE IN AN AVIATION GAS TURBINE

by

Walter William Manning

June 1987

Thesis Advisor: C. Biblarz

REPORT DOCUMENTATION PAGE

1a. REPORT SECURITY CLASSIFICATION UNCLASSIFIED	1b. RESTRICTIVE MARKINGS
2a. SECURITY CLASSIFICATION AUTHORITY	3. DISTRIBUTION/AVAILABILITY OF REPORT Approved for public release; distribution is unlimited
2b. DECLASSIFICATION/DOWNGRADING SCHEDULE	
4. PERFORMING ORGANIZATION REPORT NUMBER(S)	5. MONITORING ORGANIZATION REPORT NUMBER(S)
6a. NAME OF PERFORMING ORGANIZATION Naval Postgraduate School 6b. OFFICE SYMBOL (If applicable) Code 67	7a. NAME OF MONITORING ORGANIZATION Naval Postgraduate School
6c. ADDRESS (City, State and ZIP Code) Monterey, California 93943-5000	7b. ADDRESS (City, State and ZIP Code) Monterey, California 93943-5000
8a. NAME OF FUNDING/SPONSORING ORGANIZATION 8b. OFFICE SYMBOL (If applicable)	9. PROCUREMENT INSTRUMENT IDENTIFICATION NUMBER
8c. ADDRESS (City, State and ZIP Code)	10. SOURCE OF FUNDING NOS. PROGRAM ELEMENT NO. / PROJECT NO. / TASK NO. / WORK UNIT NO.
11. TITLE (Include Security Classification) STUDY OF ELECTROSTATIC MODULATION OF	
12. PERSONAL AUTHOR(S) Manning, Walter W.	
13a. TYPE OF REPORT Master's Thesis 13b. TIME COVERED FROM _____ TO _____	14. DATE OF REPORT (Yr., Mo., Day) 1987 June 15. PAGE COUNT 104
16. SUPPLEMENTARY NOTATION	
17. COSATI CODES FIELD / GROUP / SUB. GR.	18. SUBJECT TERMS (Continue on reverse if necessary and identify by block number) Electrohydrodynamic Spraying, Electrostatic Atomization, Gas Turbine Combustor, Combustion

19. ABSTRACT (Continue on reverse if necessary and identify by block number)

The influence of electrostatic and electrohydrodynamic charging on hydrocarbon fuel spray patterns and droplet atomization has been investigated. Research was performed in a combustion environment with an Allison T-56 combustor liner and an unmodified pressure-jet atomizer fuel nozzle. High-voltage probes and a variable-geometry probe insertion device were developed to assess the effectiveness of probe type and location on fuel spray modification and modulation. Exhaust gas temperatures and temperature profiles were measured to determine changes in the combustor's thermal profile and combustion efficiency. JP-4, JET-A and Number-2 Diesel fuels were tested to analyze electrically-assisted atomization effectiveness relative to off-design fuel performance. Net temperature increases were recorded for all fuels, yielding combustion efficiency improvements of 1.18, 1.10 and 0.68 percent for DF-2, JET-A,

20. DISTRIBUTION/AVAILABILITY OF ABSTRACT UNCLASSIFIED/UNLIMITED ☒ SAME AS RPT. ☐ DTIC USERS ☐	21. ABSTRACT SECURITY CLASSIFICATION UNCLASSIFIED
22a. NAME OF RESPONSIBLE INDIVIDUAL Professor Oscar Biblarz	22b. TELEPHONE NUMBER (Include Area Code) 408-624-5651 22c. OFFICE SYMBOL 67Bi

11. TITLE (continued) FUEL SPRAYS TO ENHANCE COMBUSTION PERFORMANCE IN AN AVIATION GAS TURBINE (UNCLASSIFIED)

18. SUBJECT TERMS (continued) Combustion Research, Electrical Spray Modification, Jet Engine Fuels.

19. ABSTRACT (continued)

and JP-4 respectively. Observations indicate electrical charging effectiveness, in terms of thermal power output per unit of electrical power input, increases in the order of JP-4, JET-A and DF-2, suggesting a direct correlation with the surface tension of the fuels.

Approved for public release; distribution is unlimited.

Study of Electrostatic Modulation of Fuel Sprays To Enhance Combustion Performance In An Aviation Gas Turbine

by

Walter William Manning
Commander, United States Navy
B.S., United States Naval Academy, 1972

Submitted in partial fulfillment of the requirements for the degree of

MASTER OF SCIENCE IN AERONAUTICAL ENGINEERING

from the

NAVAL POSTGRADUATE SCHOOL
June 1987

Author 
Walter William Manning

Approved by: 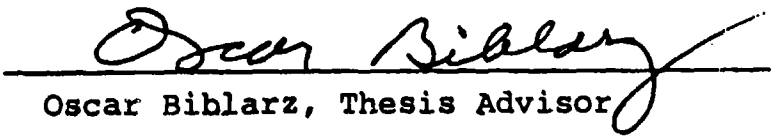
Oscar Biblarz, Thesis Advisor


M. F. Platzer
Chairman, Department of Aeronautics


Gordon E. Schacher
Dean of Science and Engineering

For
I
d
ion

A-1

ABSTRACT

The influence of electrostatic and electrohydrodynamic charging on hydrocarbon fuel spray patterns and droplet atomization has been investigated. Research was performed in a combustion environment with an Allison T-56 combustor liner and an unmodified pressure-jet atomizer fuel nozzle. High-voltage probes and a variable-geometry probe insertion device were developed to assess the effectiveness of probe type and location on fuel spray modification and modulation. Exhaust gas temperatures and temperature profiles were measured to determine changes in the combustor's thermal profile and combustion efficiency. JP-4, JET-A and Number-2 Diesel fuels were tested to analyze electrically-assisted atomization effectiveness relative to off-design fuel performance. Net temperature increases were recorded for all fuels, yielding combustion efficiency improvements of 1.18, 1.10 and 0.68 percent for DF-2, JET-A and JP-4 respectively. Observations indicate electrical charging effectiveness, in terms of thermal power output per unit of electrical power input, increases in the order of JP-4, JET-A and DF-2, suggesting a direct correlation with the surface tension of the fuels.

TABLE OF CONTENTS

LIST OF TABLES

LIST OF FIGURES

TABLE OF SYMBOLS AND ABBREVIATIONS

English Letter Symbols

A	Droplet surface area
a	semi-major axis
b	semi-minor axis
°C	Temperature, degrees Celsius
C_D	Drag coefficient
crit	Critical value
D	Droplet diameter (instantaneous)
DFM	Marine Diesel Fuel
DF-2	Diesel Fuel Number 2
ER	Equivalence Ratio (prevailing fuel-to-air ratio divided by stoichiometric fuel-to-air ratio)
e	ellipticity of a fuel droplet
°F	Temperature, degrees Fahrenheit
$F_{acceleration}$	Net acceleration force on a spherical droplet
F_{drag}	Aerodynamic drag force on a spherical droplet
$F_{pressure}$	Pressure force on a spherical droplet
F_r	Net radial force on surface of a charged droplet
H/C	Ratio of hydrogen atoms to carbon atoms
JET-A	Commercial Jet Fuel (aviation kerosene), grade A
JP-4	Military Jet Fuel, grade 4
JP-5	Military Jet Fuel, grade 5

KV	Electrical potential in kilovolts
ln	Natural logarithm
M	Mass of a fuel droplet (instantaneous)
mA	Electrical current in milliamperes
$\dot{m}_f$	Time rate of change of fuel droplet mass
mm	Distance in millimeters
N_c	Combustion efficiency
P	Pressure
PSID	Differential pressure, pounds per square inch
PSIG	Gage pressure, pounds per square inch (standard atmosphere at sea level taken as zero reference)
Q	Electrical charge
Q_s	Surface charge of a fuel droplet
r	Fuel droplet radius (instantaneous)
T_0	Combustor exhaust gas temperature, at zero probe potential
T_1	Combustor exhaust gas temperature, with electrical potential applied to probe
t_e	Total evaporation time
U	Total surface energy
U_r	Total reversible work
v_f	Velocity of fuel droplet
v_g	Velocity of gas medium surrounding fuel droplet
V_{slip}	Droplet slip velocity
We	Weber Number
Z	Ohnesorge Number

Greek Letter Symbols

α	Numerical value defined by equation 17
Δ	Numerical difference; net change in succeeding value
ϵ	Electrical permittivity
λ_B	Burning rate coefficient
λ_v	Vaporization constant
μ_f	Viscosity of fuel
μ_g	Viscosity of gaseous medium
ρ_f	Mass density of fuel
ρ_g	Mass density of gaseous medium
ϕ	Electrical field potential
σ_f	Fluid surface tension
σ^*	Surface tension defined by equation 23

ACKNOWLEDGEMENT

The author wishes to convey his sincere gratitude and appreciation to the following individuals whose contributions were essential to the completion of this thesis: Professors Oscar Biblarz and James Miller for their continuous support, guidance, and Jobian patience; Bob Besel and Ted Dunton for their exceptional technical and logistical management; Glen Middleton for his superior craftsmanship and unparalleled cooperation and professionalism; and to Commander R. G. Bettinger, USN, for his understanding and assistance in coordinating its acceptance and publication. Last but not least, a special note of thanks to Avigdor Zajdman for his willingness to share his expertise and experiences, and his everlasting encouragement and friendship.

I. INTRODUCTION

A. BACKGROUND

As world reserves of petroleum crude are being depleted, the yield of high quality crude is dwindling. Increasing shortages of high quality crude and threats of disruptions in supply caused by world economic shifts and international crises are certain to impact the availability and quality of the petroleum used to produce "mobility fuels", especially those required by high-performance military aircraft. This situation has already begun to manifest itself in the form of crude oils containing higher percentages of aromatic compounds, sulfur and nitrogen. Further, forecasts indicate that during the next two decades the only economical fuels for aircraft turbine engines will be those produced from conventional crude supplemented by forms of synthetic crude derived from sources such as shale oil, tar sands and coal [Ref. 1]. The results of these trends and the change of important petroleum properties, such as viscosity, surface tension, density, and heat content will significantly impact aviation fuels. To prepare for such changes in jet fuel quality and availability, technologies must be developed to permit the next generation of aircraft engines and fuel systems to accommodate such changes while providing superior

performance, reliability and durability. Also, since existing aircraft and current production engines will still be in the service inventories at the end of this century similar technologies must be developed to provide cost effective retrofit options for these vital assets as well.

B. OVERVIEW

The fuel controls and fuel atomization systems used in modern gas turbine powerplants are highly complex and sophisticated devices. These components have generally been optimized to provide superior performance at some critical design point while providing safe, reliable and efficient operation over the expected operating range of the engine. This is especially the case regarding the design of engines for high performance military aircraft, but it is amply important to civilian airlines and commercial operators as well, in view of their needs for cost effective performance. The research, design, and development costs of these components are a substantial portion of the design expenditure for the overall engine. Not only have these components been optimized for the required performance targets, but they have been carefully designed with a very specific "primary fuel grade that will ensure the degree of performance, safety, and reliability demanded. Significant and possibly prohibitive operational penalties accrue if engine operation is attempted on "off-design" fuels.

Generally the most immediate effect on the engine's performance caused by operation on an off-design fuel is loss of combustion efficiency caused by degradation of the fuel atomization process. The fuel nozzles are no longer able to supply the optimum droplet size and spray pattern being demanded by the engine's power controls and, at best, some degree of efficiency and fuel economy are lost attempting to regain the required power level. Under less favorable conditions, starting and altitude relight capability may be lost, while in more catastrophic cases insufficient power from an aircraft's engine may disallow a safe takeoff. Rapid power changes or radical performance demands could initiate a flameout.

To enable existing aircraft to operate under such broadened fuel specifications poses serious dilemmas to engine manufacturers and operators. Retrofitting entire fleets of aircraft demands a cost effective yet fully capable and dependable modification or replacement system to enable their continued service. However, designing and refitting such options may be too costly or moreover impossible altogether using conventional technologies. The ultimate solution to these problems may depend on new or alternative technologies that were formerly unpursued when higher fuel standards permitted conventional methods to suffice in meeting required objectives. One such

alternative technology is the altering of droplet size and spray pattern by electrically inducing a charge in the droplets through electrostatic or electrohydrodynamic methods.

Numerous researchers have investigated the electrostatic and electrohydrodynamic effects on the production or modification of liquid sprays, including hydrocarbon fuels, both theoretically and experimentally [Refs. 2-7]. Both theory and experience have shown that there are three principal effects of these technologies that could provide alternate solutions to fuel atomization difficulties. These effects are:

1. Reduction in the mean droplet size of the spray
2. Narrower droplet size distribution throughout the spray
3. Production of more geometrically defined spray patterns.

Further, it has been shown that these effects can be achieved with accelerating potentials in the range of 5-30 kilovolts, with minuscule currents of the order of 100 microamperes, and for typical gas turbine compressor geometries and fuel flow rates. These figures support the feasibility of developing, modifying or modulating jet engine fuel sprays by electrostatic devices. Moreover, they suggest the prospects of enabling the fine-tuning of the atomization quality and thermal profiles within the

combustor, thereby permitting the optimization of combustion efficiency over a wider range of operating conditions. Development of this technology could lead to the innovation of a "fire-by-wire" system of electrostatic combustion through suitable feedback and control systems utilizing high speed microprocessor techniques. This would provide, in essence, either a primary or a supplementary electronic fuel control system to provide superior power response, fuel efficiency and component durability for future generation engines while enabling service life extension of existing powerplants and aircraft. It was toward these goals that the research reported herein has been focused.

C. ELECTROSTATIC ATOMIZATION

1. Discussion

In the preceding sections the deleterious effects of operating present generation fuel atomizers outside the range of their design fuel specifications has shown that atomization quality and thence combustion efficiency would be severely penalized. Exploitation of the unique and potentially beneficial properties of electrostatic atomization could reverse this trend in existing combustion systems as a cost-effective retrofit option. Moreover, research and development in the field of electrostatic atomization could provide a subsequent generation of gas turbine engines capable of operating with impunity to the

effects of lesser grade fuels. This section will discuss the theory and practical application of electrostatic atomization and electrostatically enhanced spray atomization and modulation.

2. Theory of Electrostatic Atomization

The essence of electrostatic atomization is that a disruption of a liquid surface may be initiated by applied electrical forces resulting in the formation of charged droplets. The physics of the electrostatic disruption was first systematically examined by Lord Rayleigh during the late 1800's [Refs. 8, 9, 10]. In these works, he analyzed the phenomenon and calculated the critical charge level necessary to destabilize and disrupt a charged spherical droplet. He also observed that the resulting instability formed a liquid jet which protruded from the charged droplet. Under the continued influence of electrostatic charging, these jets were observed to breakup and form numerous small, stable charged satellite droplets. The classical statement of the Rayleigh Limit for stationary, spherical droplets follows:

a. Rayleigh Limit Criterion for a Stationary Charged Droplet

Utilizing a thermodynamics type energy balance approach, the fundamental relationships between fluid surface tension (σ_f), surface charge (Q_s), droplet surface area (A) and geometry, and the field potential (ϕ) can be

written in terms of the total reversible work (U_r) required to increase the surface area and charge of a droplet's free surface:

$$dU_r = \sigma_f dA + \phi dQ_s \tag{1}$$

Then requiring that U_r is a state function, or dU_r is an exact differential will provide:

$$\left(\frac{\partial \sigma_f}{\partial Q_s}\right)_A = \left(\frac{\partial \phi}{\partial A}\right)_{Q_s} \tag{2}$$

Further, the electric potential, ϕ, can arise from the charge associated with the droplet or from an external field influence. Then for a charged spherical droplet, with the quantity (r) being the droplet's radius, Equation (2) can be solved to determine the effect of surface charge on a surface tension. Without an external field influence, the surface charge gives rise to a potential gradient, following Coulomb's Law, that is proportional to the magnitude of the charge and inversely related to the square of the sphere's radius. This relationship is represented by the following equation:

$$\frac{\partial \phi}{\partial r} = \frac{-Q_s}{4\pi\varepsilon r^2} \tag{3}$$

where (ε) is the permittivity of the medium surrounding the droplet. And since the surface area of the spherical droplet is:

$$A = 4\pi r^2 \tag{4}$$

the differential surface area becomes:

$$\frac{\partial A}{\partial r} = 8\pi r \, . \tag{5}$$

Combining equations (2, 3, and 5) yields:

$$\left(\frac{\partial \sigma_f}{\partial Q_s}\right)_A = \left(\frac{\partial \phi}{\partial r}\right)\left(\frac{\partial r}{\partial A}\right) = \left(\frac{-Q_s}{4\pi\varepsilon r^2}\right)\left(\frac{1}{8\pi r}\right) \tag{6}$$

$$\left(\frac{\partial \sigma_f}{\partial Q_s}\right)_A = \frac{-Q_s}{32\varepsilon\pi^2 r^3} \tag{7}$$

Thus the effect of the droplet's charge on its surface tension is found by integrating (7):

$$\sigma_f = \sigma_o - \frac{Q_s^2}{64\varepsilon\pi^2 r^3} \tag{8}$$

By similar analysis the total surface energy (U) of an isolated charged droplet could be written in terms of the surface tension and the bound surface charge as:

$$U = 4\pi r^2 \sigma_f - \frac{Q_s^2}{8\pi\varepsilon r^2}. \tag{9}$$

And so the net radial force on the droplet's surface is given as:

$$|F_r| = \frac{\partial U}{\partial r} = 8\pi r\sigma_f - \frac{Q_s^2}{8\pi\varepsilon r^3} \tag{10}$$

Noting that the relationship involves the square of the charge, droplet charging of either polarity will result in a reduction in the surface tension of the droplet. Further, the effect of the charging is greatest for the smaller droplet radii, and if the magnitude to charging reaches a value such that:

$$Q_s = 8\pi(\sigma_o \varepsilon r^3)^{\frac{1}{2}} \tag{11}$$

then the drop will become unstable and eventually breakup into multiple stable droplets. This breakup condition yields the stability criterion for the minimum droplet radius capable of sustaining a specific charging level:

$$r_{min} = \frac{Q_s^2}{64\pi^2 \sigma_o \varepsilon}. \tag{12}$$

This minimum stable droplet radius is the Rayleigh Limit relationship. From this expression it may readily be deduced that the higher the level of charging, that is the greater the field intensity affecting the charging, then the larger the droplet radius at which breakup instability will occur.

b. Factors Affecting Rayleigh Limit for Nonstationary Evaporating Droplets

While the preceding classical explanation of the Rayleigh Limit adequately describes the physics of the phenomenon, it is inadequate in dealing with the physics and thermodynamics of a fuel droplet sprayed into a combustion environment. Two predominant factors that must also be considered are the fluid dynamic forces and the evaporation, or vaporization rate, experienced by the initially assumed spherical droplet. The influences of these factors, both of which tend to redefine the shape of the droplet, similarly affect the Rayleigh Limit charging and breakup mechanism. The analysis of how these bias the Rayleigh Limit for the case of nonstationary and evaporating droplets has been dealt with by Cerkanowicz [Ref. 11] and Kelly [Ref. 6]. The application of these analyses to the electrostatics of a fuel droplet spray in a combustor environment will be summarized in this section.

(1) Fluid Dynamic Factors. Practical application of electrostatic spraying or spray modulation requires analysis of the relative motion of charged fuel droplets enveloped in a gaseous medium. Consequently the initially assumed spherical droplet undergoes a deformation under the loading of fluid dynamic forces. Because of the velocity difference between the higher velocity air flow and the injected droplets, droplet drag develops. This drag provides the mechanism for distorting the droplet as well as transferring gas-phase momentum to the liquid droplets. If the droplet were initially assumed to be rigid and spherical, the droplet force balance would be simply:

$$F_{drag} - F_{pressure} = F_{acceleration} \tag{13}$$

according to Figure 1 (see Appendix B), with the velocity slip between the two phases:

$$V_{slip} = (v_g - v_f) \tag{14}$$

following the analysis given by Deane [Ref. 12].

Droplet breakup due to fluid dynamic forces in such a two phase mixture is governed primarily by the ratio of aerodynamic forces, as measured by the dimensionless group known as the Weber number (We):

$$We = \frac{\rho_g (V_{slip})^2 D}{\sigma_f} \tag{15}$$

The critical value of Weber number, We_{crit}, must be experimentally determined; but for most nonviscous fluids the value above which droplets will break up is about 12 [Ref. 13]. Similarly, the maximum droplet size which can exist in such flow conditions is:

$$D_{max} = \frac{\sigma_f \, we_{crit}}{\rho_g \left(V_{slip}\right)^2} \qquad (16)$$

In his analysis Cerkanowicz discusses the works of Taylor [Ref. 14] who approximated the effects of droplet shape distortion on the Rayleigh Limit. After a Legendre function for the first mode of drop distortion produced an ellipsoidal shape, Taylor modeled the droplet approximately as a prolate spheroid. In analogous manner to the classical Rayleigh Limit derivation of the previous section for a spherical droplet, Cerkanowicz provides for the case of a prolate spheroid the relation between surface tension and droplet charge:

$$\sigma_f = \sigma_o - \left(\frac{Q_s^2}{64\pi^2 \epsilon r^3}\right)\left(\frac{4}{NI}\right)^2 \qquad (17)$$

where: $N^2 = 2\alpha^{2/3}\,(2 - \alpha^{1/2} - \alpha^{3/2}) \,/\, (1 - \alpha)$

$\alpha = 1 - e^2$

$I = e^{-1}\ln[(1 + e) \,/\, (1 - e)]$

e = ellipticity = $(1 - b^2/a^2)^{1/2}$

a = semi-major axis

b = semi-minor axis

r = undistorted spherical radius.

By comparing the surface charge required to disrupt a prolate spheroid compared to a purely spherical droplet of the same volume, Cerkanowicz showed that the droplet distortion will cause a reduction in the charge required to initiate electrostatic droplet breakup. This supports the theory that the surface tension of a charged distorted droplet is less than the surface tension of an equally charged spherical droplet of the same volume and thus less electrostatic charging would be required to disrupt subsequently elongated droplets such as might be found in a combustor spray.

Cerkanowicz concludes his analysis by developing a unified theory for nonstationary charged droplets which relates the Weber Number stability criterion and the Rayleigh Limit criterion modified for fluid dynamic effects. In so doing, he calls upon another dimensionless group, the Ohnesorge Number, (Z), which represents the ratio

of the viscous force to the square root of the product of the inertia and surface tension forces of the fluid:

$$Z = \frac{\mu_f}{(\rho_f \sigma_f D)^{0.5}} \quad . \tag{18}$$

This he relates in the following manner to the critical Weber number. Since droplet viscosity represents the resistance of the fluid mass to the shearing action developed by aerodynamic drag forces, the Ohnesorge Number should provide a measure of the deformability of the droplet in an atomizing airstream. Therefore Z must also influence the critical Weber Number at which shattering of droplets is initiated. Citing the experimental work of Hinze [Ref. 15], shattering is found to be essentially independent of droplet viscosity at low values of Z, and We_{crit} is equal to approximately 13. At the other extreme, for large values of Z, experimental results support the theory that breakup of the droplets ceases and approximately excludes aerodynamic shattering. Hinze also developed equations relating the distortion (δ) for droplets of initial radius ($r = D/2$) upon sudden exposure to an air stream with constant relative (slip) velocity (V_{slip}). The dependence on the Weber and Ohnesorge Number is given by:

$$\frac{\delta}{r} = k(We) = \frac{k\rho_g (V_{slip})^2 D}{\sigma_f} \tag{19}$$

where:

$$k = 0.0850 \text{ for } Z \leq 1.0$$

$$k = 0.0475 \text{ for } Z > 1.0 \quad .$$

Cerkanowicz provides that for a prolate spheroid droplet the maximum distortion relative to a spherical droplet of the same volume is

$$\left(\frac{\delta}{r}\right)_{max} = 1 - \left(\frac{a}{b}\right)^{-1/3} \quad . \tag{20}$$

Then by combining Equation (19) and (20):

$$k(We) = 1 - \left(\frac{a}{b}\right)^{-1/3} \tag{21}$$

and solving Equation (17) for the ratio of surface tensions due to droplet charge:

$$\left(\frac{\sigma_f}{\sigma_o}\right) = 1 - \left(\frac{Q_s^2}{64\pi^2\varepsilon\sigma_o r^3}\right)\left(\frac{4}{NI}\right)^2 \tag{22}$$

thence, defining for clarity σ^*, the fraction by which surface tension of a spherical droplet is reduced due to surface charge:

$$\sigma^* = \frac{Q_s^2}{64\pi^2\varepsilon\sigma_o r^3} \tag{23}$$

so that:

$$\sigma_f = \sigma_o \left[1 - \sigma^* \left(\frac{4}{NI} \right)^2 \right] \quad . \tag{24}$$

It follows that the shape assumed by a charged droplet in the presence of aerodynamic force may be deduced as:

$$k(We_o) = \left[1 - \left(\frac{a}{b} \right)^{-1/3} \right] \left[1 - \sigma^* \left(\frac{4}{NI} \right)^2 \right] \tag{25}$$

with:

$$We_o = \frac{\rho_g V_{slip}^2 D}{\sigma_o} \quad . \tag{26}$$

Equation (25) is significant for it represents a unified theory for the Rayleigh Limit of droplets distorted by dynamic forces. By relating the aerodynamic force, in terms of We_o, surface tension, by σ^*, and droplet geometry through the axis ratio (a/b) it clearly defines the interdependence of these factors in determining the effects of electrostatic atomization in a gaseous flow field.

(2) Thermodynamic Factors. Since the combustion of liquid fuels in a gas turbine combustor commences with the fuel in the form of droplets, the dynamics of the droplet evaporation can significantly affect the behavior of

the atomization process. As the droplet experiences elevated temperature and beings the evaporate in the combustion environment, two important changes occur that have an influence on the effectiveness of electrostatic droplet disruption. These are the change in droplet size (and density), and the variation in surface tension of the droplet.

(a) Evaporation and Combustion. First the evaporation of the droplet causes a mass transfer as a result of the phase change occurring at the droplet's surface. As the fuel droplet vaporizes, sending gaseous phase fuel into the area surrounding the droplet, the mass of the liquid phase is reduced. Also, although in the increasing internal temperature of the remaining droplet would tend to cause it to expand, the more volatile components of the fuel are those which vaporize first, leaving behind the heavier hydrocarbons and other higher density components. This results in an offsetting of the volumetric expansion by a reduction in volume to mass ratio for the remaining droplet species. Therefore, the general effect is that of reducing the instantaneous mass as well as the size (vis-a-vis mean diameter) of the vaporizing droplet. Although a rigorous analysis of the vaporization rate and mass transfer relations is beyond the scope of this

investigation, the following simplified analysis will serve to illustrate the mechanism and physical trends.

In the evaporation of a liquid fuel droplet the rate of vaporization depends principally upon the composition of the fuel, the ambient temperature of the free stream, the medium of the free stream and the size and temperature if the droplet. Thus in order to determine the rate of vaporization it would be necessary to kno temperature gradient profiles and the composition of both the liquid and gas phases. However, if steady-state vaporization is assumed the profiles and composition for the liquid phase become inconsequential to the analysis for an assumed spherical droplet [Ref. 16]. Thus the rate of vaporization of an assumed spherical droplet will be related to its environmental factors and proportional to its (instantaneous) diameter. Either the thermal conduction or mass transfer through the gas-phase adjacent to the droplet are then the limiting factors to vaporization. The change of mass of the droplet due to vaporization may then be written:

$$\frac{dM}{dt} = \frac{\pi}{4} \rho_f \lambda_V D \qquad (27)$$

where λ_V is the vaporization constant, which is related to the material constants of the fuel and the droplet's Nusselt

Number, while D represents the instantaneous droplet diameter. Assuming average or constant values for density, ρ_f, and vaporization constant, λ_v, this preceding equation may be integrated to predict the droplet size as a function of the initial droplet diameter, the vaporization constant, and elapsed time according to:

$$D^2(t) = D_o^2 - \lambda_v t \tag{28}$$

or

$$D(t) = [D_o^2 - \lambda_v t]^{\frac{1}{2}} \tag{29}$$

where D(t) = Instantaneous droplet diameter at time (t).

This is commonly called "D^2 Law" which is especially useful in the case of mono-sized sprays but it has also been applied to a variety of droplet distribution functions by Tanasawa and Tesima [Ref. 17]. In the case of a single droplet or a mono-sized spray a plot of D^2 versus time (t) could easily be generated and the total evaporation time (t_e) would be obtained by setting D = 0 so that:

$$t_e = \frac{D_o^2}{\lambda_v} \tag{30}$$

This simplified analysis is easily extended to the case of a spherical droplet vaporizing with combustion with the following assumption. After ignition of

the droplet the surface vaporization and gas phase diffusion flame combustion sustain one another. That is, the assumption is made that the diffusion fed combustion takes place in stoichiometric proportions so that the reaction takes place instantaneously. Since chemical reactions occur "infinitely fast" in comparison to time rate of change of droplet size, this is a very reasonable assumption and further, it supports the assumption that when steady state conditions are established rate of mass vaporization is equal to rate of mass burning [Ref. 16].

The rate of mass burning, ($\dot{m}_f$), for a spherical droplet under these conditions is simply related to the rate of decrease of droplet volume according to:

$$\dot{m}_f = \frac{d}{dt}\left[\frac{4}{3}\pi\rho_f\left(\frac{D}{2}\right)^3\right] \tag{31}$$

where: m_f = mass of fuel droplet

ρ_f = density of fuel droplet.

Therefore, the time rate of change of droplet diameter may be deduced by restating the preceding in the form:

$$\frac{d(D^2)}{dt} = \frac{4\dot{m}_f}{\pi\rho_f D} \tag{32}$$

This result has been substantiated experimentally by numerous researchers [Ref. 17] and shows

that under vaporization with combustion, the droplet diameter is a function of the burning time and related to a constant λ_B called the burning rate coefficient, such that:

$$\frac{-d(D^2)}{dt} = \lambda_B \qquad (33)$$

Thus by relating Equations 28, 32, and 33, of this section for the steady state case it may be seen that:

$$\lambda_V = \lambda_B = \frac{-4\dot{m}_f}{\pi\rho_f D} \qquad (34)$$

and thus both processes, vaporization and combustion, follow the "D^2 Law" in determining the size of the droplet at any instant. It must be stated, however, that there is a functional dependence of both the vaporization constant and the burning rate coefficient on the ambient temperature of the air surrounding the droplet. The dependence is such that both increase with elevated temperature.

The important implications of reduction of the droplet's diameter due to vaporization and burning, and the acceleration of this process at elevated temperatures can have a pronounced effect on the effectiveness of electrostatics. In electrostatic applications, charge injection into the liquid may be used to form droplets or to hasten the breakup of droplets formed

by conventional atomization. The subsequent vaporization of these droplets occurs without charge loss [Refs. 6, 11] which results in an increase in the charge density of the droplet that is proportional to the vaporization constant or burning coefficient such that:

$$\frac{Q}{m} = \frac{Q}{m_o - \frac{\pi}{4}\rho_f \lambda_v (D_o^2 - \lambda_v t)^{\frac{1}{2}}} \qquad (35)$$

Thus the combined effect is to hasten the attainment of the Rayleigh Limit and initiation of droplet breakup. Roth and Kelly [Ref. 6] substantiate that the establishment of a charged droplet changes the otherwise continuous evaporative loss of mass to a process punctuated by episodes of convulsive disruption. This alteration enables each parent droplet to act as a source of highly charged sibling droplets as it evaporates and, in effect, enables each to act as an independent, electrostatically induced atomizer.

(b) Variation in Surface Tension. The second major influence of elevated droplet temperatures in the combustion environment is the effect of temperature on surface tension. The surface tension of the liquid fuel decreases approximately linearly with increasing temperature. Since surface tension of a fluid is defined as

the work done in extending the surface of the liquid one unit area, or work per unit area, the reduction in surface tension of the droplet due to elevated temperature will enhance the ability of electrostatic forces to breakup the droplet. Thus for a given droplet charge, the establishment of the Rayleigh Limit would be hastened proportionally with the increasing droplet temperature. Conversely, elevated fuel droplet temperatures would enable droplet breakup due to electrostatic effects at a correspondingly lower charge level, requiring less electrical potential than in a quiescent atmosphere. For the combined effect in the application of electrostatic atomization of spray modulation to a combustor environment, the reduction in surface tension due to increased fuel droplet temperature would augment the reduction in surface tension due to electrostatic charging and increase the probability of droplet disruption and breakup. Simply stated, elevated temperature and electrostatic charging of the fuel droplets are complementary processes influencing droplet atomization.

II. NATURE OF THE PROBLEM

A. BACKGROUND

Because of its relative simplicity and excellent potential for precision control of liquid spray production, electrostatic and electrohydrodynamic atomization has received growing attention. Electrostatic spraying has found practical application in such diverse areas as high-speed ink-jet printing, pesticide, paint and liquid metal spraying, rocket and satellite propulsion, and even fog dispersal [Refs. 2, 5, 18, 19]. More recently it has been applied to hydrocarbon fuel spraying [Refs. 2, 6, 11]. Reductions in mean droplet diameters of 20 percent to 60 percent have been reported and increases in spray-cone angle of 5 percent to 29 percent have been observed for cold spraying of hydrocarbon fuels under electrostatic influences [Refs. 3, 20]. Further, as discussed in previous sections, analysis of the effects of the combustor environment on a fuel droplet suggests that although emerging droplets may not initially be charged to their Rayleigh Limit, the processes of evaporation, combustion, aerodynamic drag and surface tension reduction should hasten the droplets passage through that limit. Thus it is reasonable to expect that electrostatic modification of fuel sprays in combustors is a

viable and efficient means by which the desired modulation and control of fuel droplet size and spray dispersion pattern can be achieved.

Consequently, a research program was established at the Department of Aeronautics, Naval Postgraduate School, Monterey, California, in 1980 to study the application of these concepts to gas turbine combustor spray atomization. In order to examine the theoretical predictions concerning the effects of electrostatic fields on combustor fuel sprays, this research has proceeded along two main paths and spanned the efforts of five thesis students. The two research paths were, first, the investigation of electrostatic spray effects on "cold" sprays produced by a combustor nozzle and second, the study of these effects under actual burning conditions in a gas turbine combustion chamber. An overview of the work of the four previous research efforts follows to provide insight into the successes and difficulties which have guided the research reported herein.

The initial research was engaged by R. J. Laib [Ref. 20]. He investigated the changes in droplet size, size distribution and spray "cone-angle" that could be induced by high voltage fields during "cold" spraying. In addition to the development of a test apparatus, his goals were to determine the reference spray patterns and droplet

size distributions produced for JP-4, JP-5 and DFM in the absence of an electrical field and observe the changes that occurred in the spray pattern and droplet size distribution when an electric field was applied. Lastly, he would attempt to electrostatically modify the spray of an alternate fuel (e.g., DFM) to resemble the spray of the reference fuel (JP-4) observed in the absence of the electrical field. The results of this research were measured utilizing high speed photography and laser light absorption techniques. With the influence of electric fields produced by a high voltage electrode positioned coaxially with the nozzle orifice, Laib was able to reduce the droplet size by approximately one-half using applied potentials of less than 30 KV. The spray of JP-5 fuel was made to resemble that of the JP-4 reference spray by the application of 29 KV. Dramatic results were also obtained with DFM under the influence of the electrical field. The spray of DFM without application of the electric field revealed droplets ranging from 600-1200 microns in diameter and a spray cone-angle of approximately 78 degrees. With a field potential of 23 KV the same measurements revealed droplets ranging from 200-600 microns and a spray cone-angle of about 90 degrees, clearly indicative of an overall improvement in the droplet size distribution and spray geometry.

The next phase of the program was conducted by L. L. Todd [Ref. 21]. The primary efforts of this phase were the design, assemblage, and evaluation of a combustor test rig capable of simulating the operational environment of a gas turbine combustion chamber. Upon completion of the test rig, electrostatic modification of the fuel spray for primary and off-design fuels was to be evaluated. The construction of the test rig was successfully completed and rudimentary measurement apparatus were put into service to correlate electrostatic effects with combustion efficiency changes. Preliminary testing of a high voltage electrode probe was then attempted. The probe entered the combustor through an existing flame propagation crossover tube opening. Two variations in probe geometry were tested. The first probe variant was insulated for passage through the combustion chamber's inner and outer walls but terminated with an exposed 90 degree bend in its stainless steel electrode. The second version used the same entry and base construction but eliminated the 90 degree bend by inserting the probe at an inclined angle. This variation permitted the addition of ceramic insulation around the formerly exposed electrode and enabled the use of purge air to offset flame holding tendencies at the exposed electrode tip. Despite these variations, neither probe was able to sustain sufficiently high voltages to produce measurable

electrostatic effects before electrical grounding of the probe occurred in combustion tests.

In a subsequent phase of the research, J. M. Logan [Ref. 22] conducted experiments along both paths, continuing the work of Laib [Ref. 20] through optical absorbtivity experiments using a "cold" spray apparatus combined with a Helium-Neon laser light source. These experiments confirmed earlier results showing that optical absorbtivity for a given fuel spray could be increased by the influence of electrostatic effects, indicating a reduction in the droplet size and, possibly, the droplet agglomeration of the sprays.

Along the second path, Logan addressed the problems of probe shorting. To attempt to overcome the debilitating effects of probe flameholding and shorting, Logan altered the design of the electrostatic probe by utilizing a spherical tipped ceramic insulator in place of the former hollow cylinder used by Todd. A small exit hole was made in the spherical tip through which the stainless steel electrode was exposed approximately 1/16-inch. By means of this design, purging air could be concentrated at the electrode tip to facilitate the reduction of flames and ionized combustion gases in the immediate proximity of this critical portion of the probe. Although three variations of this type electrode probe were investigated, all entered the combustor through the formerly used cross-over port,

inclined approximately 67 degrees incident to the combustor wall. All probes were purged with air at the tip.

With this design, Logan was the first researcher of this program to sustain a high voltage potential on the electrostatic probe within the live combustion environment. In the configuration described, the probe withstood 30 KV before arcing occurred during "cold" tests in the static combustor. Under live combustion conditions, while a peak voltage of 22 KV was recorded, the probe's electrical integrity rapidly deteriorated due to carbon deposition, and meaningful data collection was restricted to potentials of 12 KV or less, with probe currents approaching 10 mA, the maximum available from the power supply. However, unlike Todd, Logan was able to collect sufficient data to indicate that high voltage application produced measurable increases in combustor exhaust temperature. These were the fist results indicative of an increase in combustion efficiency due to electrostatic effects. It should be noted, however, that the high currents sustained in achieving these results are much higher than the "leakage" currents (which are ideally in the microampere ranges) necessary to accomplish routine electrostatic spraying. This is indicative that the electric field integrity was not being maintained continuously but instead underwent sporadic shortage-type

breakdowns to the combustion flame, gases, or grounded combustion liner.

This detriment to the maintenance of field integrity has been the major difficulty in the practical application of electrostatics to combustible sprays. Since shorting rapidly takes place when the probe is enveloped in ionized combustion gases, any flame-holding by this device exacerbates the problem. As a result of the research of Logan, it was believed that this problem might be overcome by moving the entry location for the electrostatic probe toward the nozzle end of the combustor and thus further away from the primary combustion zone or flame front. Further, it was thought that the addition of appropriate "circulation control" purging about the tip of the high voltage probe could sufficiently decrease the flame-holding characteristics of the probe itself and improve the ability to maintain a high potential between the probe tip and the fuel nozzle. These improvements were attempted during the investigations reported by J. A. Mavroudis [Ref. 23] in which this researcher participated as a co-worker.

In his research, Mavroudis investigated the improvements listed above and incorporated data measurement and recording improvements to the basic combustor test rig. As with this report, samples of test fuels were chemically analyzed by the Aerospace Fuels Laboratory, Wright-Patterson Air Force

Base, Ohio, in order that a more accurate interpretation of test data could be made. Additionally, the combustor was modified to accept electrostatic probes at the new location called, the "right-angle entry" position. This position enabled the probe tip to be placed at a distance of approximately 25 millimeters from the nozzle, entering the combustor in a radial fashion relative to the combustor's longitudinal axis. No attempts to angle the probe toward or away from the nozzle were made. The former entry port was blocked by a removable stainless steel plug.

Coincident to these modifications, the airflow facility of the test rig was calibrated to improve the accuracy, repeatability and reducibility of test data. Calibration was achieved using a standard 2.4 inch sharp edge orifice with pressure measurements taken following established procedures [Ref. 24]. Simultaneously, the pressure drop was measured across a permanent component of the test rig, namely an in-line partially closed butterfly valve (notch-type, repeatable valve). Mass flow rate was correlated for the pressure drops recorded for the orifice and the butterfly valve for a wide range of air supply valve settings. Utilizing precision manometry and a differential pressure transducer, calibration curves were produced to permit the setting and recording of airflow rates using only

the butterfly valve as a "known" pressure drop once the calibration orifice was removed.

Next a series of circulation control probes were constructed and evaluated under combustion conditions. Seven variants were tested, purging with air initially and later nitrogen. Circulation control techniques ranged from an improved end-purge probe (as used by Logan) to designs with up to five purging slots cut in various geometries around the periphery of the ceramic insulator. For those designs the maximum sustainable voltages in the combustion environment ranged from a low of about 5 KV to a high of 11.5 KV.

The results of this phase indicated that at maximum sustainable probe potentials (nominally about 10 KV) exhaust gas temperature increases of 30° F to 60° F could be achieved for some fuel-rich equivalence ratios for JP-5 and Jet-A fuels. For similar ER's using DF-2 fuel a peak temperature rise of about 100° F was recorded with a probe potential of only 9.2 KV. However, as had been the nemesis earlier, such results were obtainable only with currents of 5 to 8 mA. Also the flame holding tendency of the electrostatic probe even at its new location prchibited the maintenance of the electric field integrity at higher potentials. For fuel lean ER's which represent the normal and desirable operating condition for gas turbine combustors

the results were not as favorable. While tests of JP-5 and Jet-A fuels produced some temperature increases for potentials of 9-10 KV, key averaged only about 15° F rise. Tests of DF-2 under fuel-lean conditions produced no reportable temperature increases with voltages of approximately the same magnitude (8-10.5 KV). As before the currents required generally ranged from 5 to 8 mA.

B. RESEARCH GOALS

The primary goal of the research reported herein was to further investigate the electrostatic modulation of fuel spray patterns and atomization within the combustor. It was desired to further substantiate and assess the practicality of employing this means of increasing and controlling the combustion efficiency of gas turbine engines. Continuing the research commenced by Todd and furthered by Logan and Mavroudis, [Refs. 21, 22, and 23 respectively] this investigation concentrated upon the analysis, design, incorporation and testing of methods of maintaining a high electric field strength under actual combustion conditions. Concurrently, improvements in the methods of data measurement, recording and analysis would be pursued. Means of increasing the productivity and safety of the test rig would also be sought.

To offset the effects of the flame holding tendencies of the electrostatic probes, new designs and materials would be

investigated, and new probe variants constructed. To further reduce the effects of inserting such a "blunt-body" in the combustor flow stream, in close proximity to the primary flame zone, the design of a variable geometry probe insertion apparatus would be attempted.

This later objective had multiple purposes. First, along with suitable alignment and measuring devices, the apparatus would enable alignment of the probe's electrode precisely with the fuel nozzle's centerline, where electrostatic charging should have its most pronounced effect on the total spray pattern. Lack of such capability had caused repeatability problems during previous efforts when reinserting probes after cleaning or modification.

Secondly, a variable geometry apparatus would permit positioning the probe's electrode at varying distances from the nozzle. Moving the probe's tip along the longitudinal axis of the combustor held several advantages, the foremost being that it might allow the electrode to be sufficiently removed from the region of flame and ionized gases to preclude a shorting path. Next, as fuel type and equivalence ratios were varied, it would permit reestablishment of a non-shorting operating position. Finally, it might allow assessment of the effects of field intensity variations as a function of attainable probe voltage versus distance from the grounded nozzle.

A third benefit of a new insertion apparatus would be to facilitate precise alignment of "circulation-control" probes, since the purging slots could be oriented (with repeatability) to any angle relative to the swirl of the flow field in the combustor.

Lastly, but extremely important to this phase of the research, the new insertion device would provide for the rapid removal and replacement of electrostatic probes. This would permit not only analytical observation and cleaning of the conductive carbon deposits, but enable the analysis of new probe designs without any "down-time" to the combustor test rig itself. This later capability was extremely beneficial during the testing sequence for it permitted research to continue uninterrupted using an existing probe while a newer variant was under fabrication in the machine shop.

The most favorable results reported by Mavroudis [Ref. 23] demonstrated the ability of electrostatic spray modification for the fuel-rich case. However, such equivalence ratios are clearly not within the range where practical application of electrostatics could provide improvements in fuel economy or engine performance. Although improvements under fuel-rich conditions would assist during engine start-up and at-altitude relight, where low engine RPM's produce corresponding low compressor output

and thus higher fuel-to-air ratios, such operations are a very short and transient condition. Operations in these regimes are generally facilitated by the staging of fuel pumps and nozzle metering orifices.

Accordingly, a goal of this research effort was to concentrate on investigating fuel spray modification and combustion efficiency improvement for fuel-lean equivalence ratios, especially for the most "off-design" fuel, DF-2. It was envisioned that attainment of improvements under these engine operating conditions, where combustion efficiency is already approaching and viability of electrostatic spray modulation and control.

A final objective of this research phase relied upon the development of the previously described variable-geometry apparatus. Possessing the capability to advance the high voltage probe toward the nozzle would enable the investigation of establishing high electrical field intensities with correspondingly lower voltages as the gap between the probe and the nozzle was made smaller. The postulate that maximum practicality of electrostatic applications must be demonstrated by maximizing the droplet charging while minimizing the voltage and current required to establish the charging field defined the final objective. The use of minimal high voltage and "leakage" currents would be investigated for smaller probe-to-nozzle gaps. In so

doing it was hoped that a maximization of the ratio of thermal power output to electrical power input could be attained.

III. EXPERIMENTAL PROCEDURE

A. TEST FUELS AND PROPERTIES

Three fuels were selected for this phase of the research in order to evaluate electrostatic effects and trends over a range of physical and chemical properties. The fuels chosen included JF-4, JET-A and DF-2. Samples of each fuel were subjected to physical and chemical analysis by the Aerospace Fuels Laboratory. Wright-Patterson Air Force Base, Ohio. The results of these test (Table 1) provided the basis for accurate interpretation of the experimental data. Values for JP-5 fuel, from earlier researcher's experiments [Ref. 23] are included for comparison.

The weight-percent of hydrogen was used to calculate the stoichiometric fuel-air ratios in order to determine combustion equivalence ratios. Density was required for determining fuel mass flow from measured volume flow data. Viscosity was necessary for calibrating the fuel flowmeter and along with surface tension was valuable for predicting and assessing the quality of spray atomization and prospects for electrostatic modification. Aromatics values are shown to establish the trend that higher percentages are related to lower combustion efficiency and atomization quality. Net

Heat of Combustion figures were necessary for calculating the combustion efficiency of each fuel.

Military JP-4 (NATO SYMBOL F-40) is the design fuel for the T-56 combustor and fuel nozzle used in these tests. It is a widecut distillate fuel with high hydrogen to carbon (H/C) ratio, high net heat of combustion, and low viscosity and surface tension. These qualities give JP-4 excellent ignition, combustion, atomization, and low temperature pumpability characteristics.

JET-A is also a high grade, aviation kerosene-type fuel, but with qualities slightly less favorable than those of JP-4; it provides a "slightly off-design" comparison fuel. Preceding researchers had used military JP-5 for comparison with JET-A and DF-2. However, as analysis of the fuels reveals, JP-5 is very similar to JET-A in all respects. Additionally both JP-4 and JET-A were available locally; JP-4 at Fort Ord, California and at JET-A at Monterey Peninsula Airport. The nearest source of JP-5 was Naval Air Station, Alameda, California.

Diesel fuel, Number Two (DF-2) was also readily available through local procurement. It is the fuel used in all previous combustion tests, though Laib used marine diesel fuel (DFM) in his optical analysis. Representing the "greatly off-design" comparison fuel, DF-2 had the lowest H/C ratio and net heat of combustion values. Both indicated

DF-2 should produce relatively lower combustor temperatures and combustion efficiency for a given equivalence ratio. Its higher viscosity and surface tension predicted that DF-2 would produce poorer atomization and spray quality.

B. ELECTROSTATIC PROBES

A major portion of this research phase was dedicated to addressing the problems experienced with earlier electrostatic probes. The main undertaking was to try to minimize the obtrusive effect of the probe while maximizing its electrical charging capabilities in the "hostile" combustor environment. Considerations in designing new probes were:

1. Reduce the flame-holding characteristics
2. Maintain higher ch :ging voltage without breakdown
3. Provide high thermal and electrical insulation
4. Provide the capability for use with or without purging.

Originally the idea of using curved, insulated probe designs was considered. By utilizing a material such as quartz tubing (General Electric product "Vycor" or equivalent) it was envisioned that a curved probe insulator could be made to support the electrode in closer proximity to the fuel nozzle. In this manner it was hoped that the probe could be made more streamlined to the flow in the combustor while decreasing the electrode-to-nozzle charging

gap. However, problems immediately surfaced with this idea, not the least of which was that local fabrication facilities were not available to handle the moderately delicate process of simultaneously heat treating (in a hydrogen flame) and curving both the quartz insulator and the enclosed tungsten electrodes. Off-site contracting for such specialized, limited quantity items was also abandoned as cost-prohibitive.

Instead the manufacture of a variable geometry probe insertion device and the use of new materials was decided upon as offering the greatest overall benefit both experimentally and economically. All previous probes had been made to one fixed geometry and then rigidly mounted to the combustor outer casing, with alignment being accomplished in the machine shop; a process that precluded continuation of combustor testing when a new probe variant was being assembled. Therefore, designs were evaluated that would allow the flexibility to replace probes, change their geometry (relative to the fuel nozzle and the gas flow) and provide for alignment at the test facility instead of the machine shop. Moreover, with variable geometry the electrostatic probe could be "scanned", in terms of electrode-to-nozzle gap, in order to locate successful operating-points for electrostatic charging.

The device designed incorporated a hollow ball-joint support for a standard diameter (3/8 inch) ceramic insulator. The ball-joint was made to be self-sealing when tightened in its brass bearing-socket, while the ceramic probe was sealed by a brass washer, rubber "O"-ring and torque-nut where it entered the hollow ball-joint support on the exterior side of the device, (Figure 2).

The ball-joint allowed the probe-to-nozzle gap distance to be varied by changing the angle of the probe, fore and aft, inside of the combustor. Lateral motion of the ball-joint and extension or retraction of the probe through the hollow mount permitted precise alignment of the probe tip along the axis of the fuel nozzle. Rotation of the probe about its own axis allowed for orienting the circulation control slots of purged probes. Because of these motions, the insertion device was labeled the "four-degree-of-freedom" probe mount, (Figure 3).

To facilitate the alignment of the probe tip, a right-angle finder periscope was modified to provide a "bore-scope" along the axis of the fuel nozzle. (Figure 4). Mounted in a threaded, adjustable mounting sleeve, the periscope entered the combustor through the crossover tube port that had been used as a probe entry on earlier experiments. During preparation for combustion tests the periscope's reticle was centered on the axis of the fuel

nozzle. Next, the electrode tip of the probe was aligned exactly using the periscope's reticle. An externally mounted calibration scale was designed and constructed to provide precise and repeatable settings of the electrode-to-nozzle charging gap. With this scale, gap distances could be established in 0.5 mm increments from 5.0 mm to 35.0 mm with an accuracy of ± 0.25 mm. Once this procedure was completed, the periscope was removed and replaced by a stainless steel plug that sealed the opening in the combustion liner.

A common probe end was designed to accommodate a wide variety of candidate designs. The basic design provided a structure that could accept various probe insulation materials, provide for connection of the electrode to high voltage, and supply the capability for purging or pressurizing the probe. A cylindrical plenum was machined from stainless steel to form the end piece. At one end a 1/2 inch diameter barrel provided for cement-bonding with insulator tubes. At the other end a connector for high voltage leads was fitted. The shape of the plenum was rounded to the maximum practical extent to preclude undesirable corona discharges from degrading charging performance at the combustor end of the probe. On the side of the plenum a removable, threaded plug and "O"-ring seal were provided for connection to a pressure line. With this

common plenum end, three new probe variants were made and tested. (Figure 5)

The first variant attempted to exploit the increases in thermal and electrical insulation realized with the quartz tubing. The tubing selected was slightly less than half the diameter of the ceramic insulators used previously [Ref. 23]. Tungsten electrode rods were inserted into these tubes and then one end was turned in the flame of a small hydrogen torch. In so mating the tungsten electrode to a streamlined quartz tip it was hoped that a thinner, more aerodynamic form would offset the flame-holding difficulties while allowing the probe to function without nitrogen purging. For reference this variant was called a "sealed-quartz probe" (Figure 6).

A second design was simply a variation of the first. The tungsten-quartz seal of the first probe design proved insufficient to prevent gaseous fuel from entering the tip of the probe. As a result, the fuel entrapped within the quartz tube, would undergo thermal decomposition and form coke and soot deposits on the inside walls of the quartz. Since these deposits degraded both the electrical and thermal insulation qualitites of the probe it was decided to add nitrogen pressurization to the probe. This was not a purged probe; no attempt was made to provide circulation-control around the probe. Merely enough pressure to exclude

fuel from entering the probe tip was applied. When pressurized (to approximately 15 PSI) no flow of nitrogen could be felt at the tip, nevertheless, further fuel entrainment was prevented. This probe was called the "pressurized-quartz probe". (Figure 7)

The third design was called the "double-insulated purged probe". This probe was designed from the beginning to be purged with a flow of nitrogen, similar to the design used by Mavroudis [Ref. 23]. However, it sought to minimize flame-holding with minimal purging and reduce the distortion of the flow within the combustor. It attempted this by using smaller diameter, higher quality ceramic insulators (Coors Co., AD-998 series Alumina tubes). To provide circulation-control (to reduce flame holding at the tip) a slot approximately 1 mm wide and 5 mm long was cut into the tip of a 1/4 inch alumina tube using a diamond-saw cutting wheel. Then in order to reestablish electrode insulation in the purging slot a sheath of quartz tubing was incorporated around the tungsten electrode. This sheath was kept at the tip by spring pressure inside the ceramic insulator. In this manner the probe could be purged to provide flame blow-off at the tip without completely sacrificing electrical insulation to the depth of the purging slot (Figure 8).

C. EXPERIMENTAL APPARATUS

To provide realistic evaluation of electrostatic fuel spray modification, testing was conducted on an actual gas turbine combustor and fuel nozzle. The apparatus used in this research was the same basic equipment suite assembled by Todd [Ref. 21]. However, numerous improvements and innovations in the combustion test rig were made to provide increased accuracy and more systematic acquisition and recording of experimental data. Other changes were made to permit increased flexibility in investigating electrostatic effects, or to increase the productivity and safety of the test rig. Finally, new electrostatic probe designs and materials were incorporated to attempt to overcome the flame holding and field breakdown problems that had plagued previous research efforts. The apparatus and modifications are discussed in this section.

1. Combustor Apparatus

The combustor section consists of a single combustion liner of the type used in multiple combustor, can-annular, aviation gas turbines. The particular combustor used was a standard stock liner for Allison T-56 model gas turbine engines which power such aircraft as Lockheed C-130's (L-100) and P-3's (L-188). The T-56 liner was mounted within an eight inch diameter stainless steel pipe housing supported by a split-ring at the exhaust end,

and the fuel nozzle stem at the upstream end. Together the pipe and liner formed the entire combustor section, permitting the direction of both combustion (primary) and cooling (dilution) air through the combustor liner in a manner that closely simulated the actual engine (Figure 9). Passages extend through the pipe housing the linear to accommodate the fuel supply line and electrical igniter, as well as the electrostatic probe and alignment telescope. An air-eductor pipe with baffles receives the hot exhaust gases, mixing the exhaust with cooling air, directing it away from personnel and structures.

2. Fuel Supply System

Fuel is supplied to the combustor from a refillable, 3 liter capacity stainless steel canister. The canister is pressurized by a standard nitrogen cylinder through a pressure regulator. The delivery pressure set with the regulator determines the fuel flow rate to the combustor, while two solenoid valves ("ARM" and "FIRE") provide for pressurizing the tank and discharge of the fuel to the nozzle, respectively. A new, precision pressure regulator was added to the system to improve the stability of fuel pressure and flow rate. This regulator provided an extremely stable pressure (approximately ± 0.5 PSI) over the range 75-350 PSI required to duplicate the design specifications for the T-56 fuel nozzle.

The cylinder, canister, regulator, valves and flown meter were all mounted to a welder's cart. To improve safety aspects this cart was relocated within the concrete "blockhouse" to further protect it from a combustor fire or explosion. Lastly, a hand-operated, positive-displacement fuel pump was added to draw the desired test fuels from their respective storage barrels. The pump was mated to a large glass graduate fuel reservoir. The graduate reservoir was specifically designed and fabricated for this phase of the investigation to provide precise, repeatable measurements of fuel quantity in liters. Additionally, a preliminary fuel filter was also provided between the pump and reservoir. Together these devices contributed added precision and productivity to the test facility.

Fuel flow rates for a test could be determined (as had been done by previous researchers) by combining the duration of the test with the measured fuel quantity (volume) and the density value of the fuel. To validate this method, and improve overall data accuracy, a turbine-type fuel flow transducer and pulse converter were incorporated. A Flow Technology, Inc. Model FT-4-8 flowmeter with a Model PRC-408 converter were added to provide a real time record of fuel flow. Using manufacturer supplied universal plotting charts and data points for fluids of different viscosities, calibration curves were

made for the installed flowmeter for the range of fuels to be tested. Tests performed with the flowmeter confirmed the validity of the former methods, as the calculated and measured fuel flows repeatedly agreed within 1-percent. Chart recording of the flowmeter system's pressure regulator.

This calibration and validation later proved of great value. During a later test when the high voltage probe was allowed to arc, the high intensity electrical discharge apparently caused damage to the sensitive RF-modulator portion of the pulse-rate converter. Nevertheless, testing was allowed to continue, while awaiting a replacement unit, with assurance that the fuel system stability was consistent and reliable. While the flowmeter was unavailable, a standard in-line pressure transducer was used to provide a verification and record of fuel pressure and pressure regulator stability.

3. Air Supply System

Air flow for the combustor is supplies by an industrial grade (Carrier Brand name) 300 horsepower, vane-type compressor. The system is capable of high volume, but limited pressure due to the large diameter underground delivery piping connecting the compressor and the test facility. The combustor was immediately exhausted to atmospheric pressure through the large diameter exhaust

eductor. No attempt was made to "choke" the flow or create added back pressure on the combustor as would be found in actual engines exhausting to a gas turbine. Nevertheless, pressure drops in the range 0-10 PSI could be maintained across the combustion liner, sufficient to represent idle-power and low-power conditions for the T-56 engine.

The airflow measurement system had been calibrated during the preceding research phase as mentioned previously. The differential pressure transducer (Statham Model 12725, ± 1 psid) provided the input to a trace of a chart recorder and a digital voltmeter to enable setting and recording the pressure values which corresponded to combustor airflow rates. A flow-straightener section, used during the earlier airflow calibration, was retained to provide added flow stability to the combustor.

The calibration formulas and chart plots of pressure transducer output (volts) versus air mass flowrate generated earlier by Mavroudis [Ref. 23] were again utilized for establishing air flows for desired combustor equivalence ratios. The air supply and air flow measurement systems were both extremely stable. Overall measurement and repeatability were determined to be 4-percent or better. Calibration curve values were corrected for density changes (due to temperature variance) and for back pressure before reducing and reporting combustion test run data. A single

type-K thermocouple was used to measure combustor inlet air temperature.

Airflow control is provided by a globe valve in the air supply riser at the test facility. To provide increased operator safety and better control, the valve drive was remoted by the addition of an extension shaft and an oversized, rapid-drive control wheel. This allowed control of airflow rates from behind the concrete wall of the blockhouse instead of adjacent to the combustor test rig. The new control wheel decreased combustor over-temperature (and thermocouple burnout) by allowing airflow to be rapidly increased after combustor lightoff. It also enabled more precision in setting target airflows, with less overshoot of the desired value. Finally, it permitted the centralizing of all operating controls to one location increasing productivity and allowing two researchers to observe all data displays while safely and efficiently manning the test rig, (Figure 10).

4. Temperature Measurement and Recording

In previous efforts a single chromel/alumel (type-K) thermocouple, placed in the center of the combustor's exhaust had been used for temperature measurements. Study of gas turbine combustor literature [Ref. 25], however, led to the belief that this position alone might be insufficient to detect potential temperature variations. Also, a single

thermocouple did not provide the ability to observe temperature profiles across the combustor's exhaust plane. Consequently, a set of three inconel-shielded (but ungrounded) type-K thermocouples were installed on the combustor test rig. These were placed through the openings provided for standard service thermocouples used in actual engine applications, (Figure 11).

This arrangement allowed the thermocouples to be monitored singly or in combination. In combination, they could provide an average temperature across the exhaust plane by electrically summing their outs prior to recording on a strip chart recorder. As an added "control" temperature indicator, and as a backup sensor in case of high temperature failure of type-K device to verify changes in the exhaust profile. With the summing of the three thermocouples it was believed that a much improved representation of the average exhaust temperature, and thus the combustion efficiency, of test runs would be realized.

5. High Voltage Power Supply

The high potentials required for the electrostatic probes were supplied by a Hipotronics (Model 830-5 series) power supply capable of up to 30,000 volts output. This supply provided a variable current-limiter with a maximum capability of just over 5 mA. Voltage delivered to the electrostatic probe was recorded by a tap made parallel to

the power supply's voltmeter. To provide maximum shielding for test measurement and recording devices, the power supply received its power through an isolation transformer. Furthermore, the high voltage was supplied to the electrode through a grounded-shield coaxial cable, and the power supply was grounded to earth and the combustor test rig through separate copper braided cables. The power supply is pictured along with other test rig instruments and data recorders within the test facility blockhouse in Figure 12, while a schematic of the entire test apparatus is shown in Figure 13.

IV. RESULTS AND DISCUSSION

A. GENERAL

Summaries of significant combustion test results appear in Tables 2, 3, and 4. Overall a total of 253 separate combustion test runs were completed during which the combustor and fuel nozzle were subjected to the influence of the high voltage probes. Of this total, 71 runs wee rejected due to a defective fuel nozzle orifice, which resulted in fuel spray oscillations and unstable combustion performance (Test run 4-28-1 through 5-4-4). However, unlike previous efforts, no tests were lot due to thermocouple burnout, an accomplishment credited to the improvements made to the test facility's air supply measurement, indication and control equipment. The remainder of 182 combustion tests wee considered acceptable for data reduction and examination. Of these, the results of 55 selected test runs are presented to discuss and compare the effects observed on combustion performance in the presence of the electrostatic charging probes.

The selected results are assembles by fuel type starting with the design fuel (JP-4) then the slightly off-design fuel (JET-A) and lastly the greatly off-design comparison fuel (DF-2). To investigate the potential for improvement

in combustion efficiency as a function of probe charging-gap distances, probe-to-nozzle separation was varied from 5 to 35 millimeters. The separation used for a given test run is indicated in the column labeled "Charging gap (mm)".

Similarly, combustor inlet fuel-air mixture equivalence ratios were varied from a nominal low of approximately 0.3 to as high as 3.3. Although this research concentrated predominantly on fuel-lean equivalence ratios (ER < 1.0), some fuel rich tests (ER > 1.0) were run to validate and compare with the results of previous researchers, albeit using the latest improvements in data sensing and recording. In each case the fuel delivery pressure was maintained at a constant 90 PSIG, while a predetermined airflow rate was established to create the target value of ER desired for a particular test.

After the light-off transient subsided, the combustion temperature was allowed to stabilize; then the voltage was raised on the electrostatic probe. The voltage increase was continued to the maximum achievable without arcing (due to grounding), or to the point of high current (> 5.0 mA), whichever occurred first. The voltage was then reduced slightly to avoid a field breakdown. These quasi-peak voltage and current values are those recorded in the "VOLTAGE" and "CURRENT" columns, respectively, of the test result tables. They represent the actual "working" voltage

and current that provided the power to affect and modify the fuel spray.

The next two columns of the test results represent the average combustor exhaust temperature (TEMP), and change in combustion efficiency (ΔN_c) realized during the test run. Both values are representative of the thermal profile sensed by the thermocouple array at the exit plane of the combustor test rig. The final, "NOTES", column indicates the type of electrostatic probe used on the individual test run.

B. PROBE PERFORMANCE

The sealed-quartz probe design was the first tested. This design demonstrated the capability of quartz to materially withstand the hostile thermal environment of the combustor. It withstood the high combustion temperatures, without any form of film-cooling, from very near the nozzle (5 mm), out to the right-angle entry (25 mm) used by the previous research phase. However, the tungsten-quartz bond was insufficient to provide a gas-tight seal to prevent gaseous fuel-air mixtures from entering the probe. Thus, although it was abandoned for this reason, its use added credibility and optimism to the prospect of a follow-on pressurized quartz-tipped probe.

The pressurized-quartz probe, with a nitrogen charge of about 15 PSI, proved sufficient to prevent gaseous fuel entrainment on the interior of the quartz insulator tubing.

This probe was highly effective at preventing flame-holding, without any circulation control, for the smaller probe-to-nozzle charging gaps (up to 7.5 mm). Its thinner and more aerodynamic profile was necessary to achieve the very small charging gaps required in order to explore regions where electrostatic charging might be effected with lower voltages and currents. As the results indicate, use of the pressurized-quartz probe permitted this exploitation of the low power benefits of electrostatic charging and atomization phenomena. These data reveal increases in combustion efficiency were realized with electrical power outputs at the probe ranging from a low of 0.4 watts to a high of only 2.3 watts. A relatively impressive 1.1 percent increase in combustion efficiency was achieved for DF-2 with only 0.42 watts of electrostatic charging power expended.

To maintain appreciable high voltage on the probe beyond a distance of approximately 7.5 mm from the nozzle, it was necessary to change to a nitrogen purged probe to provide a flame blow-off counterflow around the electrode. The pressurized-quartz probe, which had performed well up to his point, became incapable of supporting voltages in excess of approximately 3.0 KV without grounding to the liner through the combustion flame. To overcome this problem the double-insulated purged probe was used to investigate charging gaps from 7.5 mm out to the maximum gap of 35 mm.

With this probe variant is was possible to continue to achieve sufficient voltages on the probe to affect the fuel spray and consequently the combustion efficiency of each fuel. Flame blow-off was provided by a 10 PSI nitrogen purge through the probe's circulation control slots. Although this alumina probe was larger and less aerodynamic than the quartz-tipped probes, the inert gas counterflow around its electrode was able to displace the flame-holding effects and enable voltages to be increased to as high as 10.5 KV on some test runs. This compares favorably with the maximum voltages achieved by Mavroudis [Ref. 23] at the right angle entry position.

Generally as the charging gap was increased the maximum voltage increased out to the 25 mm position and then tended to decrease slightly out to the maximum distance tested. This anomaly was not present during cold voltage breakdown tests where voltage increased nearly linearly with each increase in the gap distance. It is believed that beyond 25 mm, the right-angle position, the effectiveness of the nitrogen counterflow began to be offset as the electrode's potential began to be focused toward the ionized gases of the primary flame zone, instead of the fuel nozzle.

Of even greater interest was the observation that for all fuels and equivalence ratios the charging current showed a marked increase at or beyond the 15 mm gap. The reason

for this increase is believed to be attributable to a change in the electrical charging mode influencing the fuel spray. At the smaller probe-to-nozzle separations (up to approximately 7.5 mm) the modest currents indicate that the modification of the fuel spray was due largely to electrostatic charging. Here as the larger field strengths (volts-per-meter) would support, the droplets were predominantly affected through direct field emission in the relatively higher local electric fields focused upon the nozzle. At the greater probe-to-nozzle separations, the order of the magnitude increase in the charging current strongly suggests that the fuel spray was being influenced by electrohydrodynamic charging. In this case, the fuel spray was being influenced by electrohydrodynamic charging. In this case, the fuel spray modifications were being affected by the creation of a corona discharge about the tip of the probe; fuel droplets passing through the region of the corona's influence were then electrically accelerated in their breakup process relative to the amount of acquired electrical charge.

Finally, and for both the electrostatic and electrohydrodynamic cases, a general trend was observed when the charging power was examined for the various test runs. This examination indicated that the power (wattage) required to achieve changes in the fuel spray was greatest for JP-4,

less for JET-A, and least for DF-2. The reason for this is believed to be that the more optimal the fuel, the better the natural atomization of the fuel nozzle (smaller, more stable droplets), and consequently the more power (or work) required to effect a reduction in the surface tension of the mean droplet size in the spray.

C. COMBUSTION EFFICIENCY

Energy analysis of a standard combustor reveals that for a given fuel type (i.e., constant heat values) and constant equivalence ratio (i.e., steady fuel and air mass flow rates), the combustor's thermal efficiency determined solely by the amount of heat addition realized between the inlet and outlet of the combustor. Provided the equivalence ratio contains excess combustion air, then any process which causes an increase in the combustion reaction, during the residence time of a given mass of fuel-air mixture within the combustor, would result in an increase in the combustor's thermal efficiency. An improvement in the fuel spray quality or the atomization efficiency of the fuel nozzle are examples of the processes that would allow this increase in the combustion efficiency.

The numerical value of a combustor's thermal efficiency can be calculated from its air and fuel mass flow rates, the ...mal property constants for the fuel (net heat of combustion and specific heat values) and the temperature

change across the combustor. The efficiency then becomes simply the ratio of combustor thermal energy output to the chemical energy input available for conversion to thermal energy. A change in combustor efficiency, for a given, steady-state, set of fuel and air parameters can be reduced to simply the net relative change in combustion temperature:

$$\Delta N_C = \frac{T_1 - T_0}{T_0} = \frac{\Delta T}{T_0} \qquad (36)$$

where T_0 = Average exhaust temperature before voltage application

T_1 = Average exhaust temperature after voltage application

Calculations of the actual combustor thermal efficiency were made for various equivalence ratios with the electrostatic probe inserted, but without high voltage applied [Ref. 26]. Examination of these curves revealed that, for the fuel-lean case, the design fuel. JP-4, provided combustion efficiencies from approximately 88 to 98 percent as the ER decreased from about 0.45 to 0.30, respectively. Correlation of these plots revealed that the ordering of combustion efficiency, in descending order was JP-4 followed by JET-A, and then DF-2. While the plots were nearly identical, in terms of parallel slopes at any given ER, JET-A's combustion efficiency was consistently 0.5 to

1.5 percent lower than JP-4; similarly, DF-2 was consistently 5 to 6 percent lower than the design fuel.

To detect changes in combustion efficiency caused by the effects of high voltage application required a sensitive yet stable temperature sensing system. This was provided by the electrical summing and averaging of the three type-K thermocouples that were laterally spaced at the exhaust plane of the combustor. Together these thermocouples provided a very stable temperature trace, which virtually eliminated random and nonhomogeneous thermal fluctuations from appearing in the temperature recordings. The overall noise factor was reduced by greater than 70 percent relative to a single centrally located type-K thermocouple used in earlier investigations. Simultaneous recording of the constancy of fuel and air flow rates provided further assurance that changes in the average temperature profile during high voltage application were directly related to the electrical charging influence of the probe on the fuel spray.

Favorable results in affecting the exhaust temperature were recorded for all three fuels. Significant increases in combustion efficiency (0.3 percent or greater) were produced in 54 of the 182 acceptable combustor test runs. The significant results for JP-4 ranged from 0.35 to 0.68 percent, with an overall average combustion efficiency

increase for all tests of 0.56 percent. The range for JET-A was more favorable with combustion efficiency increases from 0.30 to 1.10 percent and an average increase of 0.66 percent. The most impressive results were those for the "well off-design" fuel, DF-2, ranging from 0.38 to 1.10 percent, with the highest overall average of 0.77 percent combustion efficiency increase for all significant test runs.

While these percentages may seem small on first consideration, it must be realized that the baseline combustion efficiency is fairly high. In the case of JP-4 the average baseline combustion efficiency is approximately 93 percent for the range of equivalence ratios tested. Thus, even in the ideal case, the maximum combustion efficiency increase achievable for JP-4 is only 7.0 percent. Consequently, the average increase of 0.56 percent realized for JP-4, the design fuel, is in fact 8.0 percent of the absolute efficiency increase remaining for an ideal combustor.

Other indications of the probe's electric field influence were also observed. Although not all tests in this research series made net positive changes in the average exhaust temperature, most tests did produce a lateral variation of the exhaust temperature profile. For example, during some tests a temperature decrease was

recorded on the side of the combustor opposite the probe, while increases were recorded on either or both the central and the other side thermocouple. On other instances an increase in temperature was recorded on the central thermocouple with no change or a decrease in temperature on the two side thermocouples. In no instance, however, was there an overall decrease in the temperature profile, nor a net loss in the average exhaust temperature observed.

The best example of this phenomena detected a 36° C variation on an average profile temperature of approximately 880° C. Taken as a simple ratio, this observation indicates a temperature "modulation" of over 4 percent. It is believed that, either singly or in combination, the repulsion of like charged fuel droplets and the attractive force created by the high potential of the probe's electrode were responsible for this observed nonuniformity across the exhaust plane.

Analysis of the combustion efficiency results by fuel type indicates that the more off-design the fuel, the greater the degree of combustion efficiency enhancement achievable. Not only did the overall maximum change in combustion efficiency increase as the results were examined for JP-4, JET-A and DF-2, in that order, so too the overall average of the changes in combustion efficiency likewise increased. These findings also corresponded with the

observed trend that the power (wattage) required to achieve combustion efficiency improvements decreased in the same order JP-4, JET-A and DF-2. Simply stated, with all other factors equal, for a given electrical input power one would expect greater combustion improvement for DF-2 than for JP-4. Again, the cause for these observations is believed to be related mainly to the relative magnitudes of the surface tension of the three fuels.

One other observation worth comment is that combustion improvements appear to be realizable only for a narrow range of equivalence ratios. The reasons for this are believed to be at least two fold, mainly the relationship between ER and the position of the flame-front in the combustor, and the relationship between ER and the size of a typical droplet. First, as ER changes the region affected by the flame-front and ionized gases also changes, moving longitudinally along the combustor's axis. At low equivalence ratios this region is believed to move upstream toward the fuel nozzle. Thus at lower ER's achieving sufficient probe gap to maintain a high potential relative to the fuel nozzle, in comparison to the breakdown potential to the flame front or flame-holding areas, becomes a limiting factor. This condition is exacerbated by the short residence time and higher stability of the smaller, higher-speed droplets.

As ER is increased appreciably another limit is reached where the larger droplet size requires more work than can be provided by the electrical field at its maximum sustainable voltage. The droplet residence item in the field's influence is too brief to cause droplet breakup. For fuel-rich equivalence ratios, the flame front has moved even further downstream. Following the previous analysis, the relatively lower air flow velocity has allowed the mean droplet size to remain even larger. However, now the droplet size is so large that its stability is very low and consequently the achievable electrical influence is sufficient to cause its breakup. Finally, another upper limit is reached where the droplet size is so large that the electrical power achievable is insufficient, relative to the droplet's residence time in electrical field's influence, to measurably hasten the droplet's breakup.

V. CONCLUSIONS

1. Hydrocarbon fuel spray patterns can be modified and modulated by the influence of an electrical field. The electrical field effects can be applied to an existing, unmodified fuel nozzle by a relatively simple, inexpensive and low power fuel droplet charging system.
2. In the presence of an electrical field the atomization quality of a fuel nozzle (e.g., the mean droplet diameter) and the geometry of the spray (e.g., the spray cone-angle) can be modified in a manner that favorable affects the average exhaust gas temperature of the combustor.
3. Increases in the average exhaust gas temperature can be induced by electrical field influences on the fuel nozzle and spray. These increases produce proportional increases in the net combustion efficiency of the associated combustor.
4. Two mechanisms of electrical droplet charging, electrostatic and electrohydrodynamic, appear to have been demonstrated using the same combustor and electrical charging system. In each instance changes in the combustor's exhaust temperature profile were detected during the presence of the electrical field.

5. Of the two charging mechanisms, the electrostatic case appears to hold the greatest prospects for improving a combustor's combustion efficiency and correcting temperature variations at its exhaust plane. In this case, small probe-to-nozzle charging gaps permitted relatively low voltages and leakage currents to produce significant effects on the spraying of all fuels tested.
6. Electrostatic charging provided the greatest net power conversion increase for each of the three fuels tested. For JP-4 the maximum combustion efficiency increase-per-watt of electrical power input was 1.45%-per-watt with a driving electrical potential of only 4.0 KV; for JET-A, 1.84%-per-watt with 4.4 KV; and for DF-2, 2.62%-per-watt with 4.2 KV.
7. Electrohydrodynamic charging produced considerably lower net power conversion increases than the electrostatic case. For JP-4 the maximum combustion efficiency-per-watt of power input was 0.017%-per-watt with a driving potential of 9.0 KV; for JET-A, 0.031%-per-watt with 8.0 KV; and for DF-2, 0.066%-per-watt with 8.0 KV.
8. There appears to be a correlation between the fuel type and the amount of the electrical power required to induce significant combustion efficiency increases or temperature variations. In both charging mechanisms the

power requirements tend to increase by fuel type in the order DF-2, JET-A, and JP-4. This suggests that power requirements vary inversely in relation to the surface tension and viscosity of the fuel.

9. The reason for the correlation between power requirements and the fuel properties is believed to be that the higher the surface tension and viscosity the poorer the normal atomization provided by the fuel nozzle. Thus the nozzle yields a larger, less stable, mean droplet size. This distribution of droplet sizes, in turn, requires less electrical charging power (or work) input to effect the reduction in surface tension necessary to hasten the breakup of the mean droplet size in the spray.

10. The apparatus utilized and the results achieved should be interpreted mainly as an experimental demonstration of electrostatic and electrohydrodynamic principles. They should not be interpreted as a maximized system nor as approaching the practical limits of the phenomena. The gains realized should be viewed as substantiating the desirability of continued research and prototype development in conjunction with other advances in combustion technology such as ceramic combustor materials and electronic fuel control systems.

APPENDIX A: TABLES 1-4

TABLE I

PROPERTIES OF TEST FUELS

	JP-4	JET-A	DF-2	JP-5
Hydrogen (wt %)	14.1	13.4	12.3	13.3
Density (kg/m^3)	755	822	870	827
Kinematic Viscosity (cst at 16°)	1.03	2.1	8.0	2.2
Surface Tension ($N/m \times 10^{-3}$ at 20°C)	23.5	25.6	28.8	--
Aromatics (volume %)	14.1	18.9	67.0	22.7
Net Heat of Combustion (MJ/kg)	43.4	43.0	42.4	42.9

TABLE 2

SELECTED TEST RESULTS

FUEL TYPE: JP-4

RUN#	CHARGING GAP (mm)	ER	VOLTAGE (KV)	CURRENT (mA)	TEMP (°C)	$+\Delta N_C$ (%)	NOTES
3-18-04	7.0	0.391	4.5	<0.5	890	0.56	1
3-18-06	7.0	0.410	4.4	<0.5	940	0.53	1
4-21-13	7.5	0.402	4.4	<0.5	942	0.63	1
4-21-14	7.5	0.362	4.0	<0.5	877	0.35	1
4-26-04	7.5	0.362	4.0	<0.1	868	0.58	2
5-17-10	15.0	0.338	6.0	<0.1	843	0.77	2
5-17-11	15.0	0.316	6.0	<0.1	801	0.56	2
5-17-16	20.0	0.446	8.0	4.5	997	0.50	2
5-17-17	20.0	0.396	8.0	4.5	917	0.55	2
5-17-18	20.0	0.380	8.0	4.5	900	0.55	2
5-17-19	20.0	0.345	8.0	4.5	836	0.48	2
5-18-01	25.0	0.380	9.0	5.0	884	0.56	2
5-18-02	25.0	0.345	9.0	5.0	826	0.60	2
5-18-03	25.0	0.437	10.5	5.0	976	0.55	2
5-18-16	30.0	0.360	9.0	4.5	883	0.68	2
5-20-01	35.0	0.395	10.0	4.5	900	0.44	2
5-20-02	35.0	0.358	9.0	4.5	855	0.60	2

NOTES: (1) Pressurized - Quartz Probe
(2) Double-Insulated Purged Probe

TABLE 3

SELECTED TEST RESULTS

FUEL TYPE: JET-A

RUN#	CHARGING GAP (mm)	ER	VOLTAGE (KV)	CURRENT (mA)	TEMP (°C)	$+\Delta N_C$ (%)	NOTES
4-07-04	5.0	0.443	4.4	<0.1	929	0.81	1
4-07-10	5.0	0.393	4.6	<0.1	935	0.53	1
4-21-07	7.5	0.380	4.0	<0.1	923	0.30	1
4-21-10	7.5	0.360	4.1	<0.1	845	0.60	1
4-21-11	7.5	0.392	4.6	<0.5	922	0.40	1
4-21-12	7.5	0.355	4.6	<0.5	858	1.05	1
5-17-07	15.0	0.333	8.0	>1.0	836	--	2
5-17-20	20.0	0.440	8.0	4.5	1002	0.50	2
5-17-21	20.0	0.390	8.0	4.5	896	0.60	2
5-17-22	20.0	0.411	8.0	4.5	959	0.80	2
5-17-23	20.0	0.377	8.0	4.5	904	1.10	2
5-18-05	25.0	0.394	9.5	5.0	908	0.60	2
5-18-06	25.0	0.357	9.5	5.0	859	0.90	2
5-18-07	25.0	0.456	9.0	4.5	1019	0.40	2
5-19-02	30.0	0.347	9.5	4.5	826	0.90	2
5-20-04	35.0	0.420	9.0	4.5	959	0.41	2
5-20-05	35.0	0.336	9.0	4.5	818	0.61	2

NOTES: (1) Pressurized - Quartz Probe
(2) Double - Insulated Purged Probe

TABLE 4

SELECTED TEST RESULTS

FUEL TYPE: DF-2

RUN#	CHARGING GAP (mm)	ER	VOLTAGE (KV)	CURRENT (mA)	TEMP (°C)	$+\Delta N_C$ (%)	NOTES
4-15-08	5.5	0.329	4.0	<0.1	825	0.90	1
4-21-02	7.5	0.340	4.2	<0.1	837	1.10	1
5-20-14	7.5	0.380	6.0	<0.2	883	0.91	2
5-13-09	9.5	0.347	4.0	0.2	758	1.12	2
5-13-11	9.5	2.44	4.0	5.0	1113	1.05	2
5-17-12	15.0	0.452	8.0	<2.0	968	0.40	2
5-17-13	15.0	0.390	8.0	<2.0	850	1.06	2
5-17-14	15.0	0.370	8.0	<2.0	836	0.50	2
5-17-25	20.0	0.406	8.0	4.5	900	0.67	2
5-17-26	20.0	0.363	8.0	4.5	843	0.59	2
5-17-27	20.0	0.330	8.0	4.5	80[illegible]	0.65	2
5-18-10	25.0	0.396	9.0	4.5	883	0.75	2
5-18-11	25.0	0.385	9.0	4.5	799	1.17	2
5-18-12	25.0	0.304	9.0	4.5	761	1.18	2
5-18-13	25.0	2.73	8.0	4.5	1045	0.48	2
5-19-03	30.0	0.407	9.0	4.5	867	0.62	2
5-19-04	30.0	0.328	9.0	4.5	765	0.87	2
5-19-05	30.0	0.420	8.0	4.5	875	0.63	2
5-19-06	30.0	0.338	8.0	4.5	774	0.65	2
5-20-07	35.0	0.290	8.0	4.5	705	0.43	2
5-20-08	35.0	0.322	8.0	4.5	743	0.38	2

NOTES: (1) Pressurized - Quartz Probe
(2) Double - Insulated Purged Probe

APPENDIX B: FIGURES 1 THROUGH 13

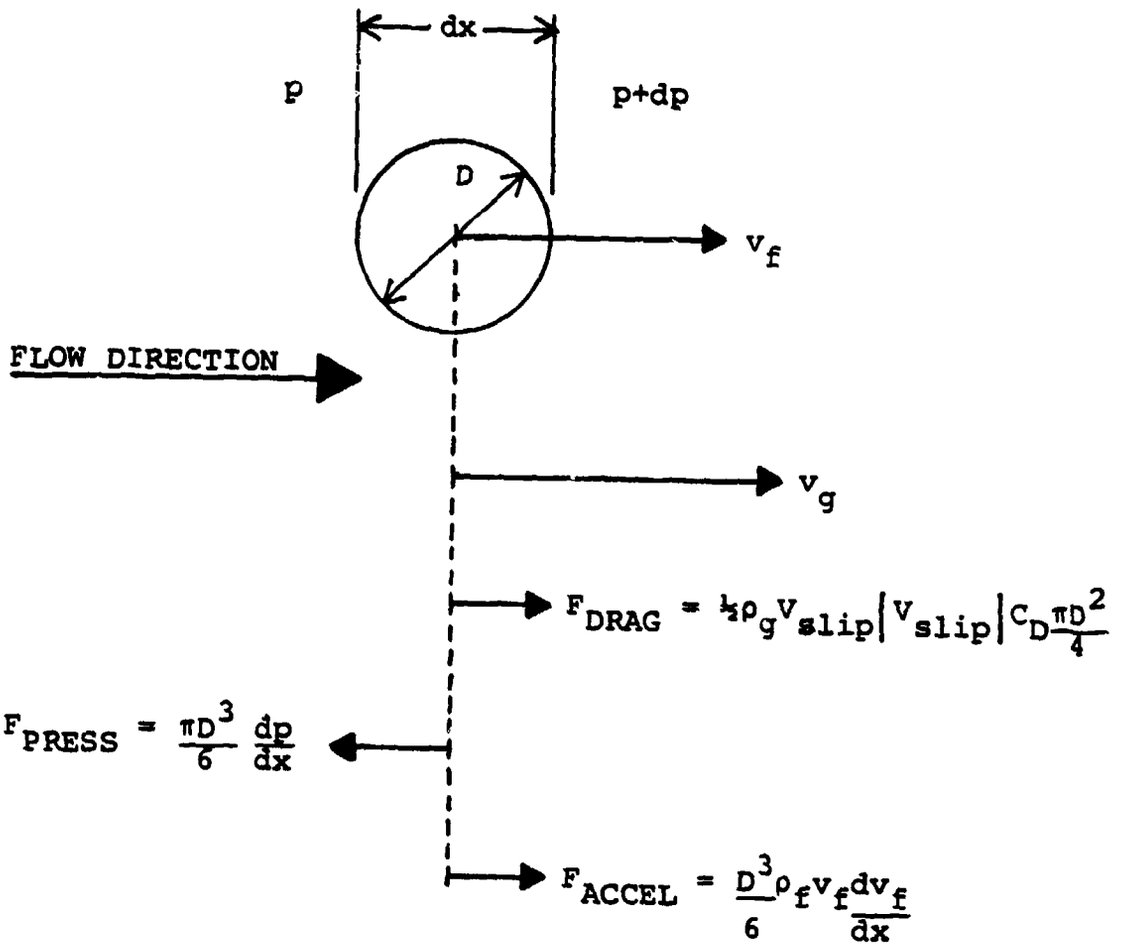

$$F_{DRAG} - F_{PRESS} = F_{ACCEL}$$

Figure 1. Fuel Droplet Force Balance

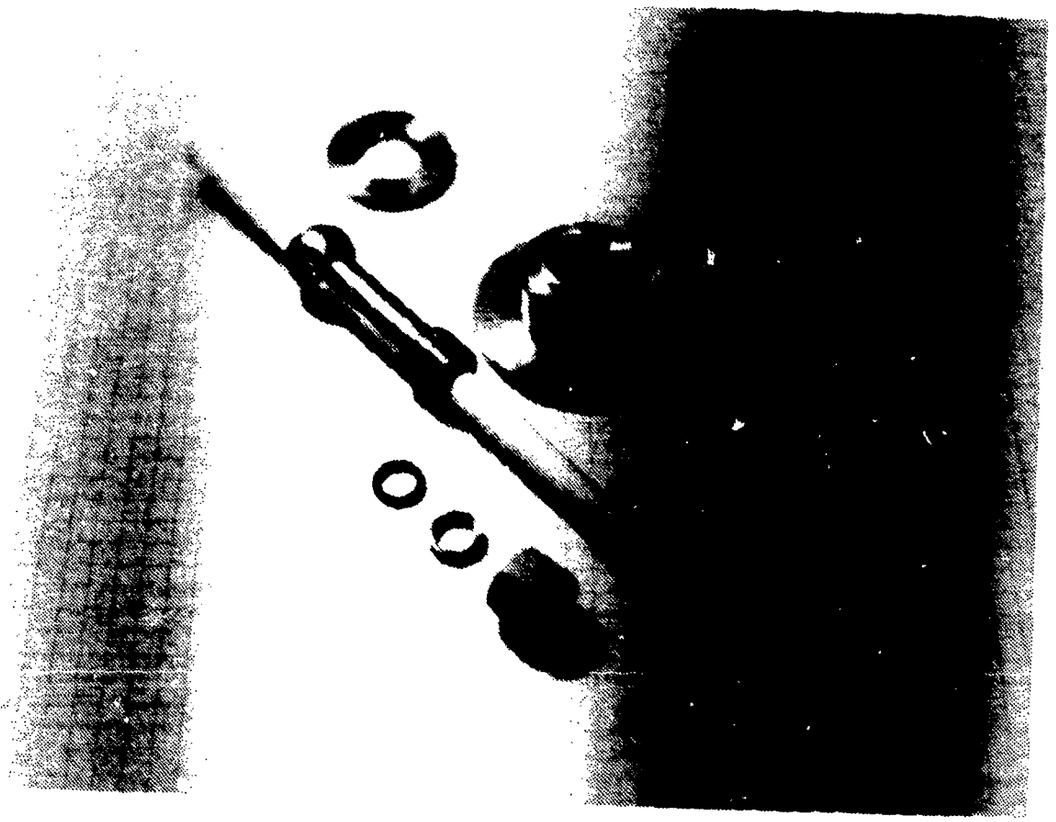

Figure 2. Hollow Ball-Joint Support for Electrostatic Probes

Figure 3. Four-degree-of-freedom Probe Mount and External Calibration Scale

Figure 4. Probe Alignment Periscope

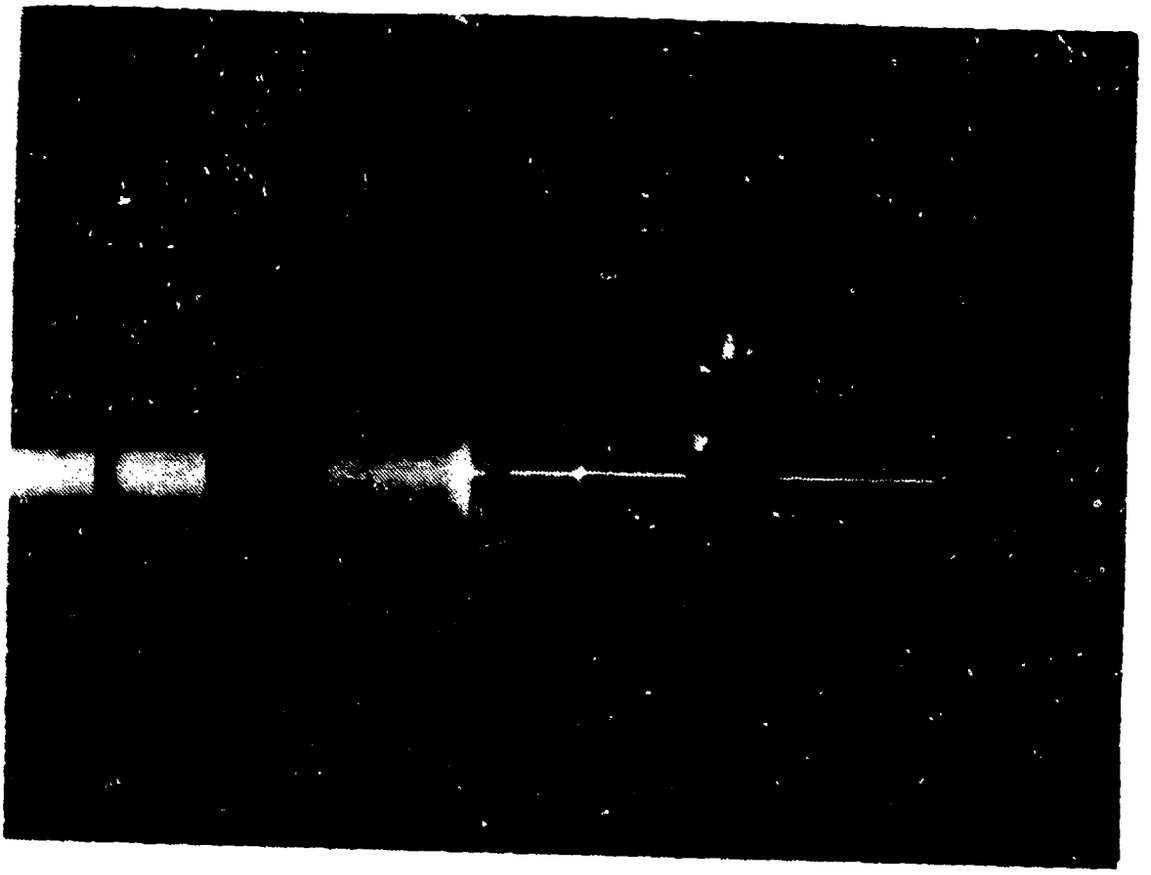

Figure 5. Common Probe End Cylindrical Plenum

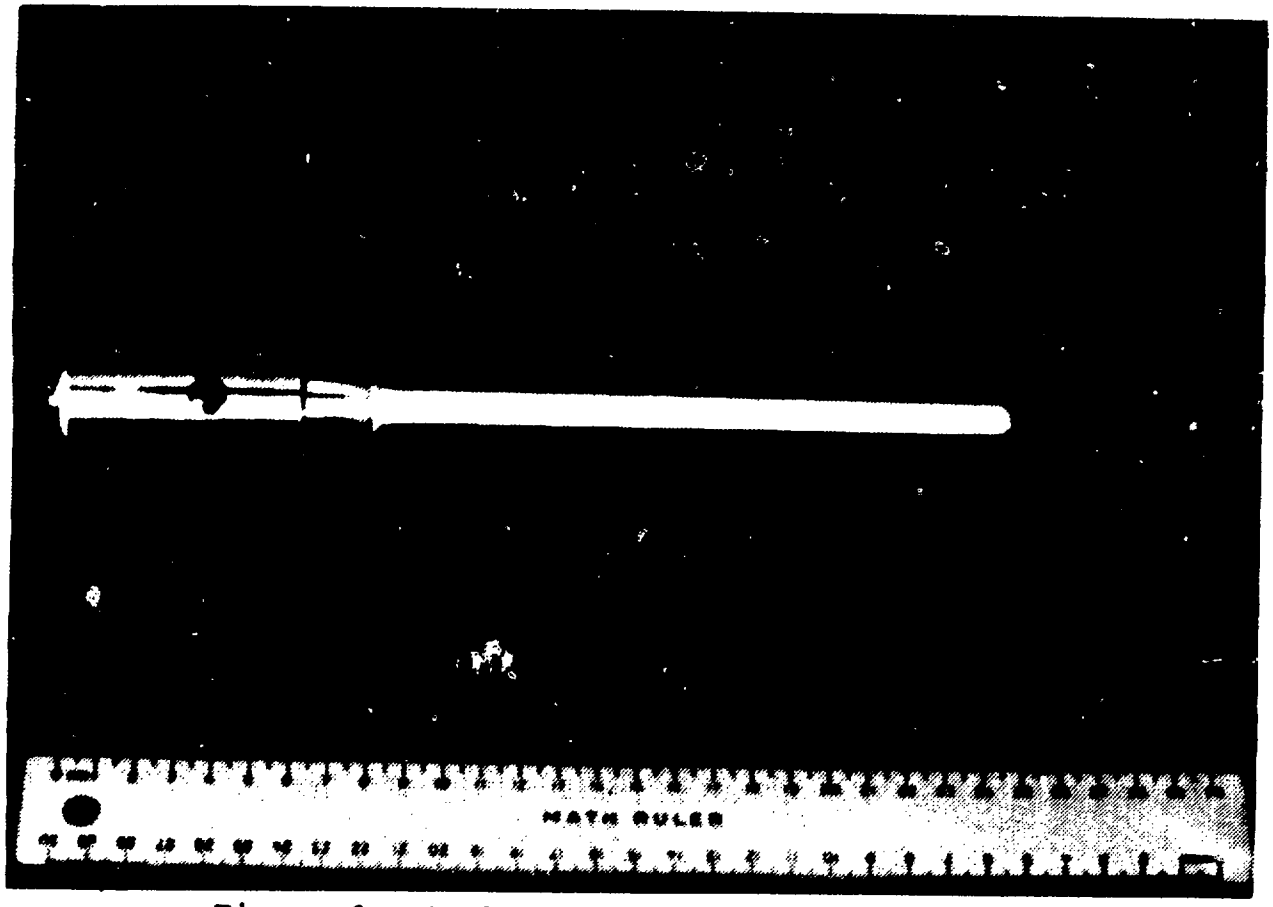

Figure 6. Sealed-quartz Electrostatic Probe

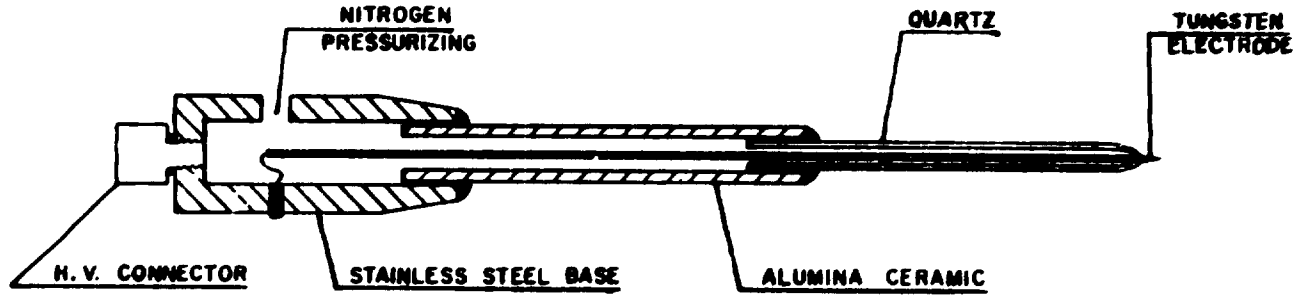

Figure 7. Pressurized-quartz Electrostatic Probe

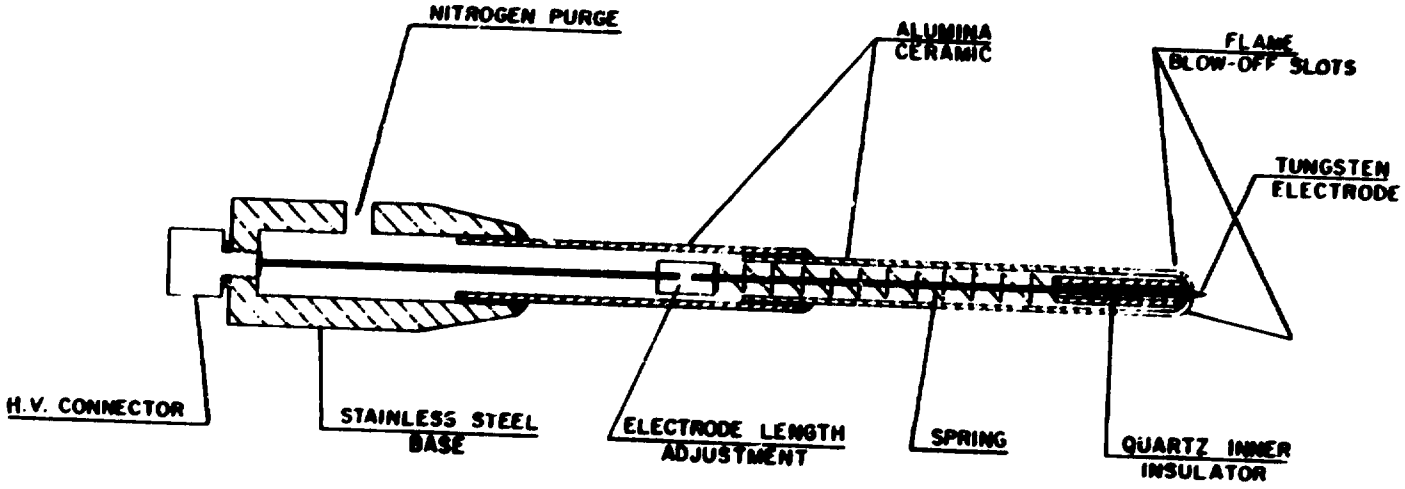

Figure 8. Double-insulated Purged Electrostatic Probe

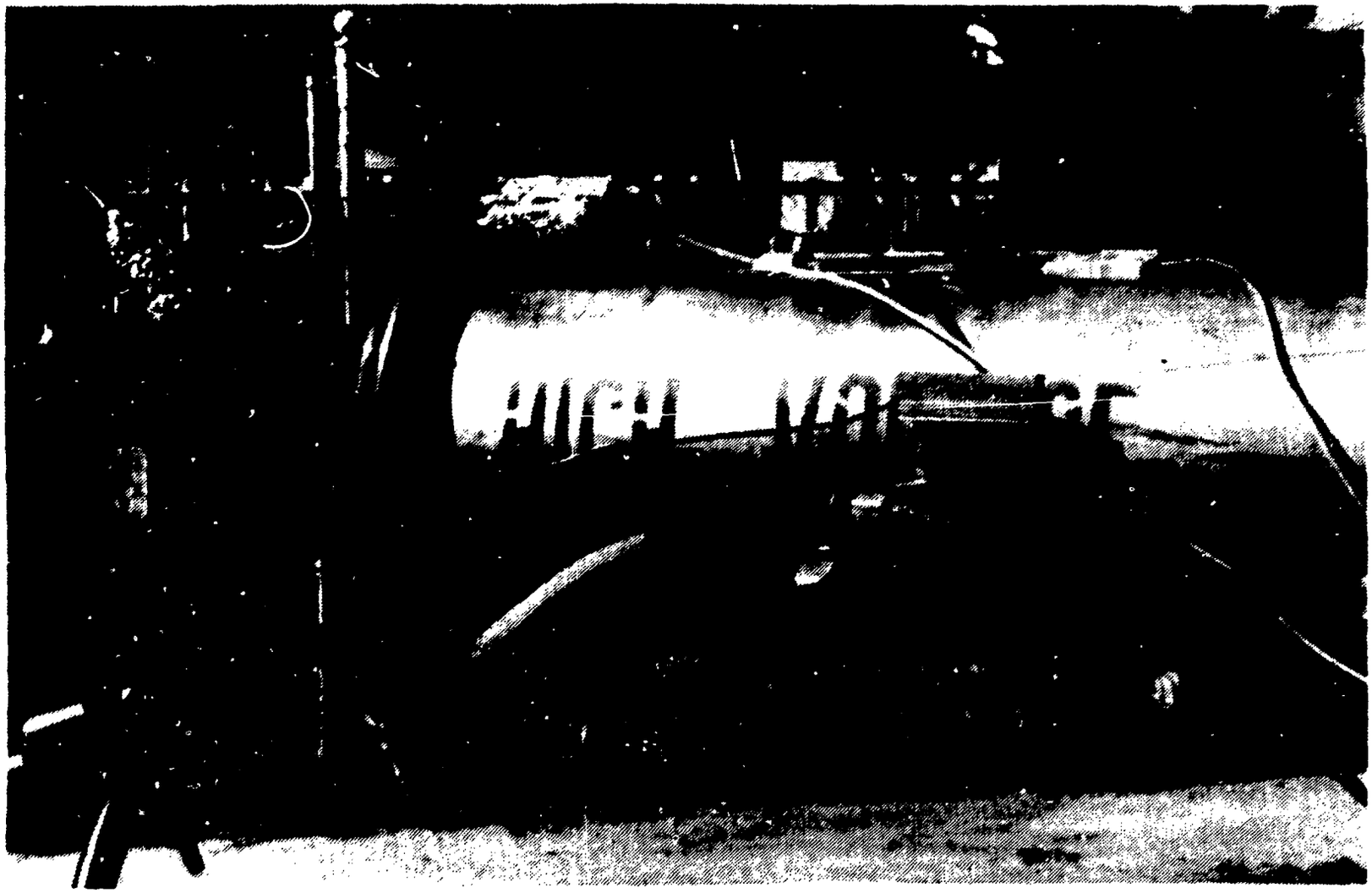

Figure 9. Combustor Test Apparatus

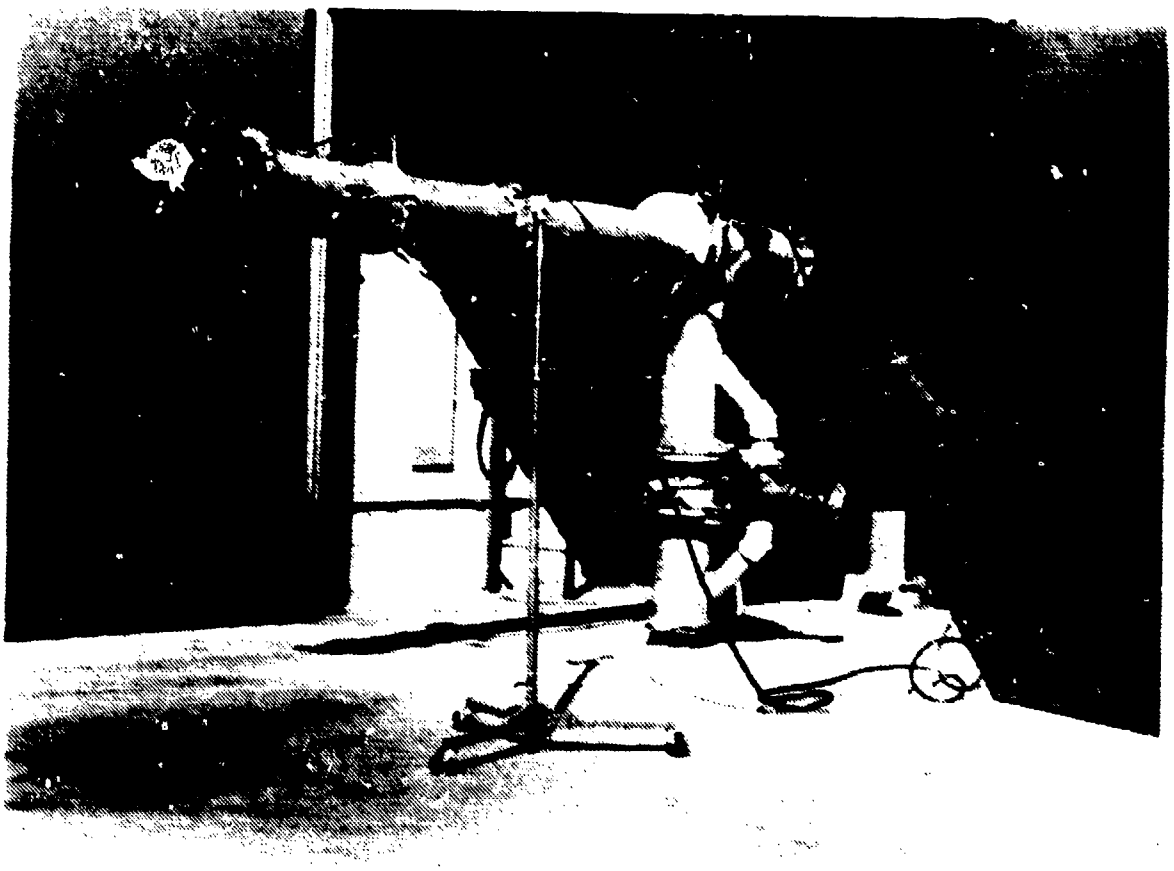

Figure 10. Combustion Air Supply

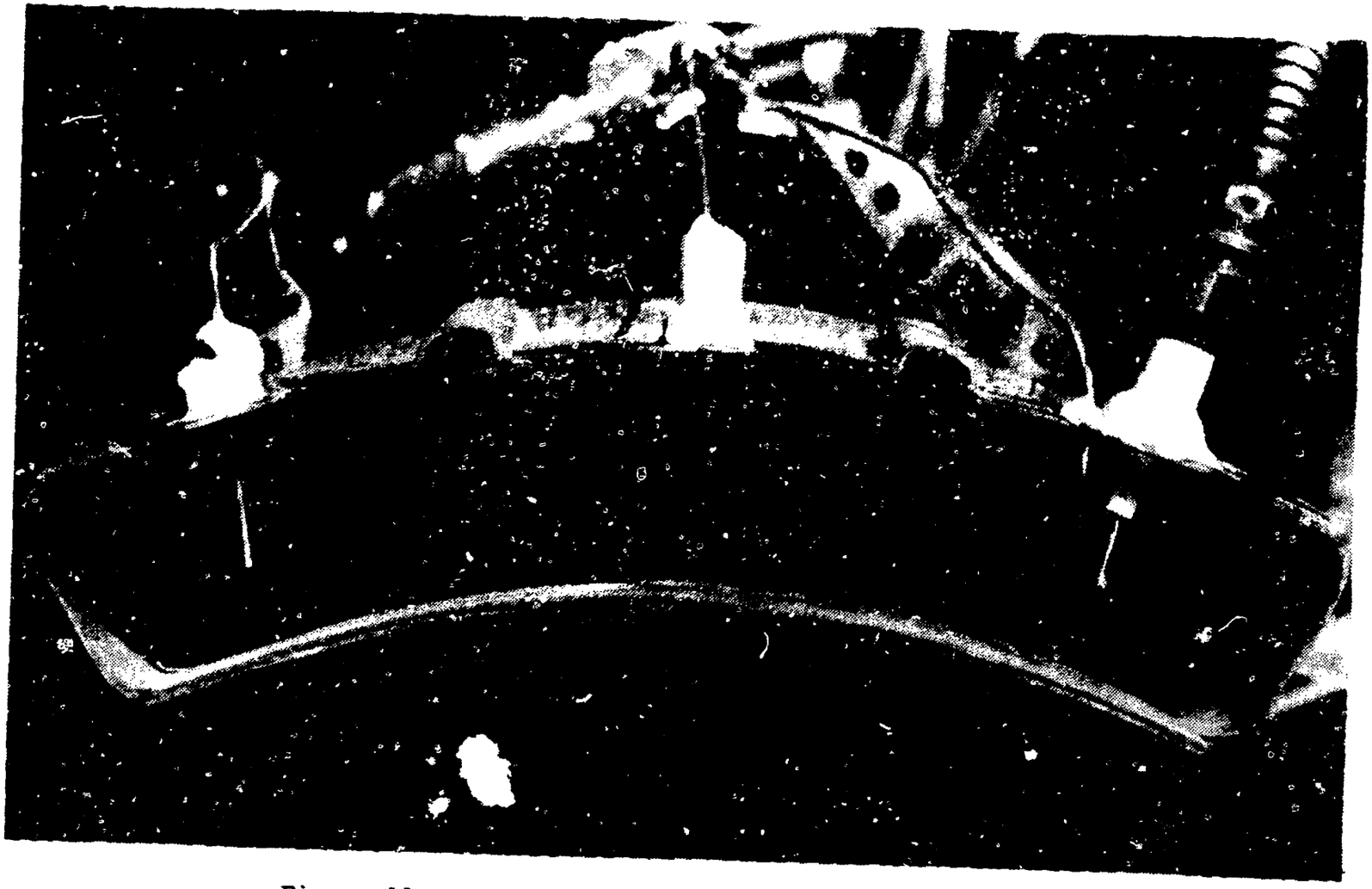

Figure 11. Combustor Exhaust Plane Thermocouple Array

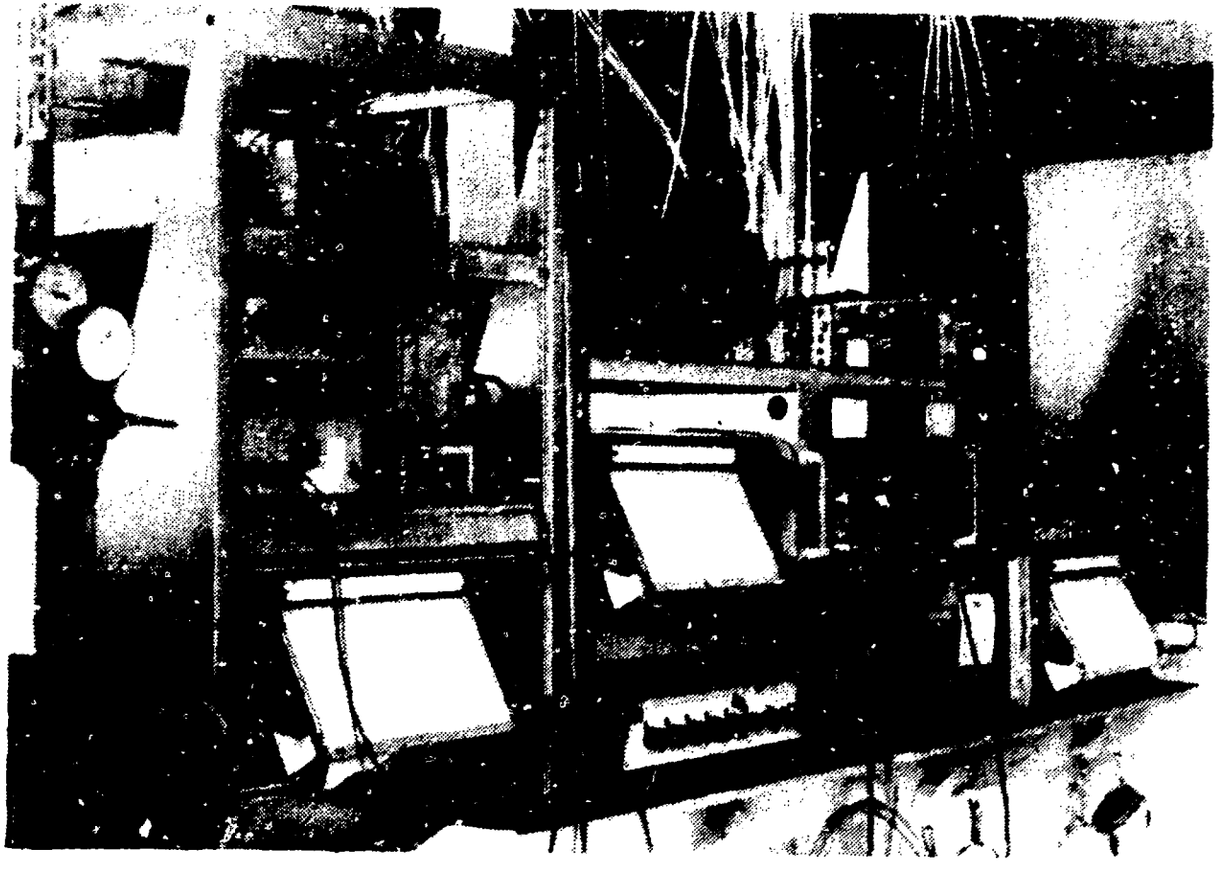

Figure 12. Combustor Test Rig Instrumentation, Recording and Operation-Console

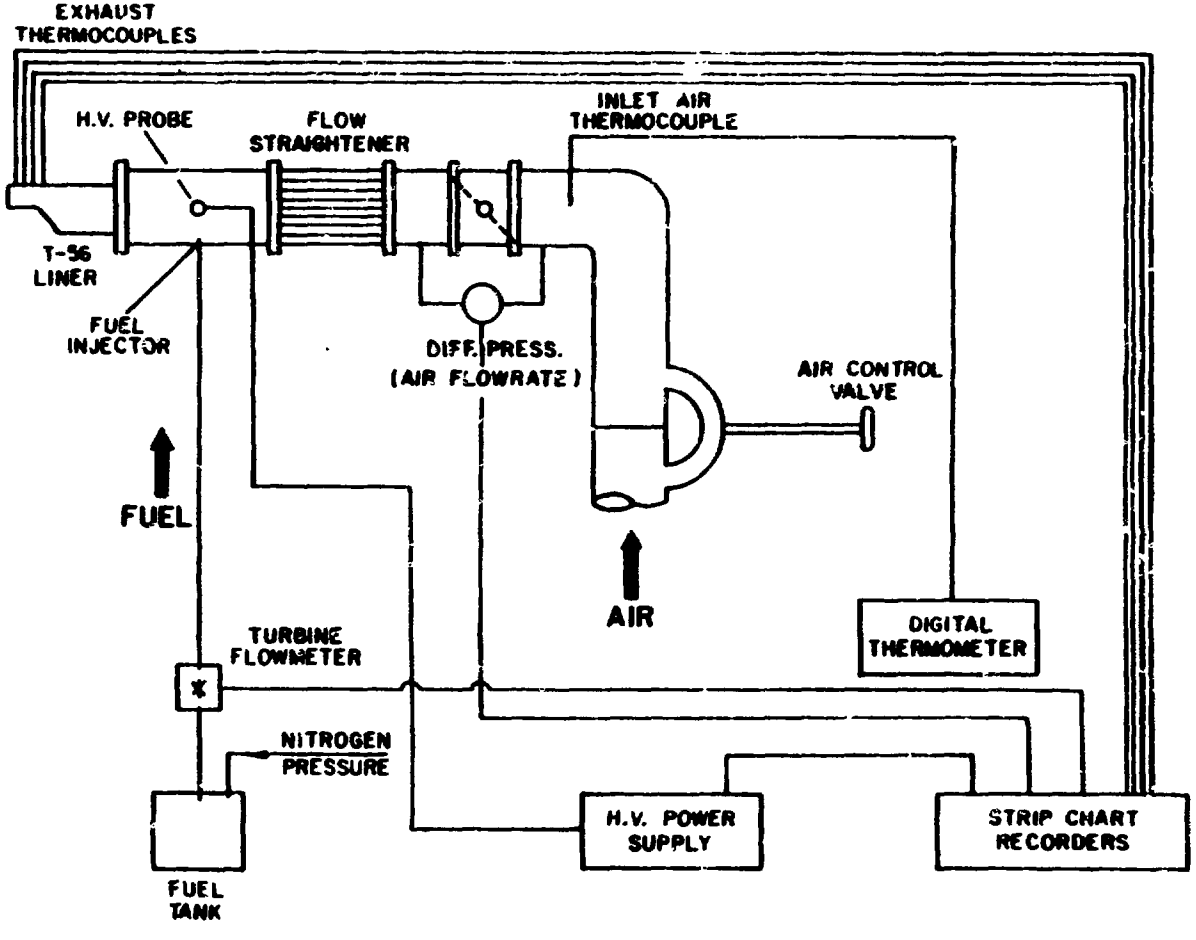

Figure 13. Combustor Test Apparatus, Schematic Diagram

LIST OF REFERENCES

1. AGARD Advisory Report No. 181, Propulsion and Energetics Panel Working Group 13 on Alternative Jet Engine Fuels, Vol 1, Executive Summary, by Whyte, R. B., ed., p. 1, July 1982.

2. Kelly, A. J., The Electrostatic Atomization of Hydrocarbons, paper presented at the 2nd International Conference on Liquid Atomization Systems, Madison, Wisconsin, June 20-25, 1982.

3. Ito, K., Yamane, K., and Fudazawa, S., "Electrostatic Atomization of Liquid Fuels," Journal of Fuel Society of Japan, V. 51, pp. 721-732, September 1972.

4. Jones, A. R., Thong, L. C., "The Production of Charged Monodisperse Fuel Droplets by Electrical Dispersion," Journal of Physics: Applied Physics, V. 4, pp. 1159-1166, 1971.

5. Robinson, K. S., Turnbull, R. J., and Kim, K., "Electrostatic Spraying of Liquid Insulators," IEEE Transactions of Industry Applications, V. IA-16, No. 2, pp. 308-317, March/April 1980.

6. Roth, D. G. and Kelly, A. J., "Analysis of the Disruption of Evaporating Charged Droplets," IEEE CH1575-0/80/0000-098, pp. 998-1013, 1980.

7. Pfeifer, R. J. and Hendricks, C. D., "Charge to Mass Relationships of Electrohydrodynamically Sprayed Liquid Droplets," The Physics of Fluids, V. 10, pp. 2149-2154, October 1967.

8. Rayleigh, J. W. S., "On the Instability of Jets, " Proceedings of the London Math Society, V. X, pp. 4-13, 1878.

9. Rayleigh, J. W. S., The Theory of Sound, V. 2, Dover Publishing Co., 1845.

10. Rayleigh J. W. S., "On The Equilibrium of Liquid Conducting Masses Charged With Electricity," Philosophical Magazine, V. 14, No. 5, pp. 184-186, 1882.

11. Cerkanowicz, A. E., Rayleigh Limit for Nonstationary Charged Droplets, paper for Exxon Research and Engineering Company, Linden, New Jersey.

12. Naval Research Reviews, V. XXXIV, A Working Theory of Two-Phase (Gas-Liquid) Flow, Office of Naval Research, Arlington, Virginia, by C. W. Deane, et al., pp. 47-50, 1982.

13. Wallis, G. B., One-Dimensional Two-Phase Flow, pp. 376-378, McGraw-Hill, 1969.

14. Taylor, G., "Disintegration of Water Droplets in an Electric Field," Proceedings of The Royal Society of London, V. 280, pp. 283-397, 1964.

15. Hinze, J. O., "Forced Deformations of Viscous Liquid Globules," Applied Science Research, V. A1, pp. 263-272, 1976.

16. Kanury, A. M., Introduction to Combustion Phenomena, pp. 145-172, Gordon and Breach, Science Publishers, Inc., 1975.

17. Williams, A. F., Combustion of Sprays of Liquid Fuels, pp. 65-67, Paul Eleck, Ltd., 1976.

18. Kelly, A. J., "Electrostatic Metallic Spray Theory," Journal of Applied Physics, V. 47, No. 12, pp. 5264-5271, December 1976.

19. NASA Contractor Report 36[illegible], Test Results of Modified Electrical Charged Particle Generator for Application to Fog Dispersal, by Frost, W., and Huang, K. H., 1983.

20. Laib, R. J., Design of an Apparatus for the Study of Electrohydrodynamic Control of Spray From Fuel Injectors in Gas Turbines, Engineers Thesis, Naval Postgraduate School, Monterey, California, December 1982.

21. Todd, L. L., Design of an Apparatus for the Study of Electrostatic Effects on Gas Turbine Fuel Sprays and Combustor Efficiency, Master's Thesis, Naval Postgraduate School, Monterey, California, September 1981.

22. Logan, J. M., Electrohydrodynamic Spraying Modifications of Aviation Fuels in a Gas Turbine, Master's Thesis, Naval Postgraduate School, Monterey, California, June 1982.

23. Mavroudis, John A., Experimental Study of Electrostatically Modified Fuel Sprays on Gas Turbine Combustor Performance, Master's Thesis, Naval Postgraduate School, Monterey, California, December 1982.

24. Flow Measurement, Chapter 4, pp. 1-80, American Society of Mechanical Engineers, 1959.

25. Swithenbank, J., et al., "Three-dimensional Two-phase Mathematical Modelling of Gas Turbine Combustors," published in Gas Turbine Combustor Design Problems, Hemisphere Publishing Corp., 1980.

26. Zajdaman, Avigdor, Electrical Spray Modification with Various Fuels in a T56 Combustor. Contractor Report, NPS-67-83-003CR, Naval Postgraduate School, Monterey, California, March 1984.

INITIAL DISTRIBUTION LIST

		No. Copies
1.	Defense Technical Information Center Cameron Station Alexandria, Virginia 22304	2
2.	Library, Code 0142 Naval Postgraduate School Monterey, California 93943-5002	2
3.	Department Chairman, Code 67 Department of Aeronautics Naval Postgraduate School Monterey, California 93943	1
4.	Associate Professor O. Biblarz, Code 67 Bi Department of Aeronautics Naval Postgraduate School Monterey, California 93943	4
5.	Professor J. Miller, Code 67 Mo Department of Aeronautics Naval Postgraduate School Monterey, California 93943	4
6.	CDR Walter W. Manning Air University PSC #1 Maxwell AFB Montgomery, Alabama 36112	2
7.	Commanding Officer Naval Air Systems Command Attn: Mr. G. Derderian, Code AIR 330B Attn: Mr. Tom Momiyama, Code AIR 330 Washington, DC 20361	2
8.	Dr. Alan Roberts Headquarters, Naval Material Command Energy and Natural Resources Research and Development Officer Navy Department Washington, DC 20360	1
9.	Mr. C. D. B. Curry, Patent Counsel Office of Naval Research One Hallidie Plaza, Suite 601 San Francisco, California 94102	1

10. Dr. Lloyd Back
Fluid Dynamics and Reactive Processes Group
Jet Propulsion Laboratory
4800 Oak Grove Dr.
Pasadena, California 91109 — 1

11. Dr. A. J. Kelly
Department of Mechanical and Aerospace
Engineering
Princeton University
Princeton, New Jersey 08544 — 1

12. Mr. C. L. Delaney
Airforce Aero Propulsion Laboratory
Wright Patterson Air Force Base, Ohio 45433 — 1

13. Mr. R. A. Rudey
NASA Lewis Research Center
2100 Brookpark Road
Cleveland, Ohio 44135 — 1